Nonresonant interaction of high-power optical radiation with a liquid

F. V. Bunkin and M. I. Tribel'skiĭ

P. N.. Lebedev Physical Institute of the Academy of Sciences of the USSR
Usp. Fiz. Nauk 130, 193–239 (February 1980)

Various aspects of the problem of nonresonant interaction of high-power optical radiation with a liquid are discussed. The nonlinear response of the liquid to a pulse of radiation that significantly affects the thermodynamic state of the liquid (in particular, transforms the liquid into the vicinity of the critical point) is described. Specific features of boiling of the liquid under the action of the laser radiation are pointed out. The instability of the planar vaporization front, arising from the action of radiation on the free surface of an absorbing liquid, with respect to small spatiall perturbations of the phase separation boundaries and the perturbations of the temperature distribution related to them are analyzed. The generation of sound pulses and monochromatic sound waves in the liquid,, as a result of the action of laser radiation, and their transformation with subsequent propagation are described. The efficiency of "thermal" and "striction" mechanisms for photoexcitation of sound are compared. The phenomenon of deep melting penetration (dagger-shaped penetration zone) of metals under the action of laser radiation,, related to the presence of a liquid phase (metallic melt) in the interaction zone, is discussed. The resullts of studies concerning the interaction of high-power light fluxes with metallic targets are presented. It follows from these results that within a well-defined range of laser radiation intensities a metal-dielectric transition occurs in the interaction zone, but the appearance of the dielectric phase has no qualitative effect on the nature of the interaction.

PACS numbers: 79.20.Ds, 64.70.Fx, 78.20.Hp

CONTENTS

"I made a very important discovery in the bathtub," said Mr. Morkou, without any embarassment. "V-very, v-very important!" nodded the dog approvingly. "We discovered that water is v-very, v-very wet."

Gianni Rodari, The Adventures of Chipollino

1. INTRODUCTION

a) Purpose of the review

Almost immediately following the creation of the first lasers, when experimentalists had access to devices that were capable of generating electromagnetic radiation with a degree of coherence that had not been seen until that time, and, of focusing it into small volumes, creating enormous flux densities, the basic directions for the development of the physics of the interaction of laser radiation with matter were clear. At this time, most of the studies concerning nonresonant interaction simply involved the use of the highest possible radiation flux densities for acting on matter. Later, with the creation of picosecond lasers, studies concerning the response of matter to ultrashort high-power pulses of radiation were also included. There is no need to list here all the essentially new effects that were discovered. It is sufficient to mention such effects as self-focusing, optical breakdown in dielectrics, the nonlinear photoelectric effect in metals, multiphoton ionization of gases, and so on.

With all of this work, we, "without any embarrassment," take the liberty to assert that many phenomena that arise with nonresonant interaction of laser radiation with matter, the study of which does not require the highest possible radiation intensities or the shortest possible pulse durations, have either been studied inadequately or not at all. Apparently, this can be

*Translator's note: The literal Russian terminology refers to a molten "dagger-shaped" zone penetrating deep into a metal.

 0038-5670/80/020105-29$01.10

explained by the fact that each successive accomplishment in laser technology (the creation of new types of lasers, increase in the output power of existing types of lasers, and so on) provided such wide possibilities for carrying out essentially new research that this unavoidably led to some reorientation on the part of specialists, possibly, to the detriment of research that had become traditional.

Such problems, undeservedly bypassed by specialists, include first of all various phenomena arising from the action of high-power light fluxes on a liquid. These phenomena, as a rule, have no similarities with the action of radiation on matter in other aggregate states, which makes their study especially important. This review is devoted to discussing some problems taken from this area. We have attempted, as far as possible, not to dwell on problems that have been discussed previously in one way or another. Chapter 4, which concerns the generation of sound by laser radiation and the accompanying phenomena, is an exception (due to the importance of the problem and the large number of new results obtained recently).

b) Basic notation

The content of the review is interrelated by the overall subject matter. However, we attempted to make the presentation in such a way that each chapter, if necessary, could be read without using the material from the rest of the review. For this reason, we considered it useful to present here a list of the basic notation used throughout the review. We use the following notation below.

A is the absorptivity of the liquid surface ($0 \leq A \leq 1$); A_m is the atomic weight; C is the specific heat capacity; c is the speed of light in a vacuum; K is the absorption coefficient for radiation (cm^{-1}); N_A is Avogadro's number; p is the pressure; q is the flux density of optical radiation; r_0 is the radius of the focal spot; T is the temperature, which is measured everywhere in energy units; u is the speed of sound; v is the specific volume; $\alpha = (1/v)(\partial v/\partial T)_p$ is the coefficient of volume expansion; $\beta = -(1/v)(\partial v/\partial p)_T$ is the isothermal compressibility; $\varkappa$ and χ are the coefficients of thermal conductivity and thermal diffusivity, respectively ($\chi = \varkappa v/C_p$); λ is the specific heat of vaporization; $\rho = 1/v$ is the density; and τ is the duration of the laser pulse.

In addition, unless otherwise stated, the index "0" everywhere denotes the initial (equilibrium) value and the index "C" everywhere denotes the critical (relative to the liquid-vapor transition) value of the corresponding quantities, while a prime denotes their deviation from the initial or equilibrium values. The remaining notation is introduced in each chapter independently and is used only within that chapter.

2. OPTOTHERMODYNAMIC PHENOMENA IN A LIQUID

Apparently, one of the most important problems in optothermodynamics from the practical point of view is the problem of strong compression and heating under the action of a laser pulse of a predetermined shape. This problem has been formulated and studied within the framework of the problem of laser-induced fusion (see the review in Ref. 1 and the literature cited therein). However, this is not, by any means, the only problem in which a macroscopic system is transformed from a given initial state into a given final state along a prescribed path under the action of high-power optical radiation (the problems that constitute the subject of optothermodynamics[2] can be briefly described in this manner).

In particular, there is considerable interest in the optothermodynamic problems that concern the interaction of radiation with a liquid. Problems that are related with different types of phase transitions, will be examined separately in view of their particular importance, (see Chapters 3, 6). Here, we shall concentrate on studying those cases for which the curve that encloses the phase volume of the system, (the region of allowable values of thermodynamic variables) subjected to the action of radiation, is located entirely within a single-phase region.

One of the first problems within this group is the problem concerning the transition from the normal state (p_0, ρ_0) into the vicinity of the critical point (p_1, ρ_1), which was examined in Ref. 2. This problem is solved most easily in the case that the transition occurs along isobar and isochore segments. Let the laser radiation be focused onto the free surface of a liquid and let the following inequalities be satisfied: $r_0 \ll L, r_0 \ll K^{-1}$, where L is the length of the neck of the caustic. Then, in order that there would not be enough time for the pressure in the focal volume to drop, the duration of the laser pulse τ_1 must satisfy the inequality $\tau_1 \ll r_0/u$ (in the more general case, r_0 must be replaced in this inequality by the smaller of the quantities r_0, L, K^{-1}).

Let us note that the technically simplest case, when the transition occurs according to the scheme $(p_0, \rho_0) \to (p_0, \rho_1) \to (p_1, \rho_1)$ [in this case, the shape of the laser pulse along the $(p_0, \rho_0) \to (p_0, \rho_1)$ branch can be arbitrary, provided that its duration satisfies the inequality $\tau \gg r_0/u$], cannot be realized, since the liquid unavoidably gets into a metastable region along the $(p_0, \rho_0) \to (p_0, \rho_1)$ branch, and begins to boil. The effects stemming from such phenomena will be discussed in Chapter 3.

One of the possible variations in the phase trajectory is the transition $(p_0, \rho_0) \to (p_1, \rho_0) \to (p_1, \rho_1)$. The transition $(p_0, \rho_0) \to (p_1, \rho_0)$ is brought about by a short laser pulse $\tau_1 \ll r_0/u$ with an arbitrary shape. Estimates show that the liquid usually is not heated significantly in this region (the typical heating is several degrees). The transition from the state (p_1, ρ_0) to the final state (p_1, ρ_1) occurs under the action of a shaped laser pulse. The shape of the pulse is chosen in such a way that the drop in pressure, caused by the removal of stress in the focal volume into the unperturbed liquid, would be compensated by an increase in p due to an absorption of radiation. Most of the heating of the liquid occurs in this region. In this case, the duration of the pulse

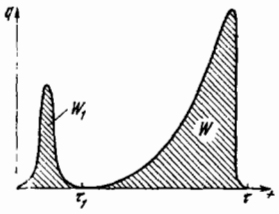

FIG. 1. An example of the shape of a laser pulse that, by acting on the free surface of a liquid, transforms the liquid in the focal spot into the vicinity of the critical point.

must be of the order of r_0/u, while its intensity must increase monotonically, in view of the increase in the heat capacity $C_p(p_1, \rho)$ and decrease in density ρ.[3]

The approximate shape of the entire laser pulse is illustrated in Fig. 1. Numerical estimates for ethyl alcohol ($T_C = 521$ K; $p_c = 69$ bar; $\rho_c = 0.27$ g/cm^3) for a transition from the normal conditions ($p_0 = 1$ bar, $\rho_0 = 0.815$ g/cm^3) into the supercritical region $p_1 = 70$ bar, $\rho_1 = \rho_C$, $T_1 = 525$ K with $K = 0.5$ cm^{-1} and $r_0/u = 4.10^{-7}$ s give a temperature increment $\tau' = 3.4$ K on the isochore branch, an energy $W_1 = 0.1$ J for the short laser pulse, and a total pulse energy of $W = 20$ J.

In this manner, the energy parameter examined lie within the limits accessible to very modest laser technology that is available today, and in an actual laser setup, the criterion for optimality should not be the condition for minimum laser pulse energy, but the possibility for predetermining the pulse shape.

Other possible problems in optothermodynamics include the generation of high-power pressure pulses having a given shape in a liquid, the study of induced critical opalescence, (i.e. brought about by the same radiation that transforms the liquid into the vicinity of the critical point) and so on.

The examples of optothermodynamic problems presented above concerned the situation in which the sound excitation has enough time to encompass only a small part of the entire liquid within the time of the radiation pulse, ($u\tau \ll V^{1/3}$, where V is the total volume occupied by the liquid). In this case, the problems of optothermodynamics can be solved, generally speaking, only with the use of laser pulses that have a particular predetermined shape, which presents additional difficulties for performing the appropriate experiments.

However, another formulation of the problem is possible. Let the liquid completely fill a volume, enclosed by a thermally insulated airtight solid cuvette that is transparent to the radiation. In this case, for sufficiently long pulses ($u\tau \gg V^{1/3}$), independent of the relationship between V and the size of the focal volume, the energy in the laser pulse is "spread out" by the sound waves throughout the entire volume V, and in addition, there is no further loss in energy due to the conservative nature of the system. Since pressure gradients are smoothed out with the speed of sound, for at $u\tau \gg V^{1/3}$, the pressure will have a smooth component, depending only on the time, on which weak spatial-temporal "ripples" will be superposed. These ripples are caused by the interference of sound waves that are generated in the liquid as a result of the absorption of radiation and they are multiply reflected from the walls of the cuvette. Neglecting these "ripples," it may be assumed that the pressure in the given case is only a function of the time elapsed from the beginning of the radiation pulse and is the same at all points inside cuvette at any fixed moment in time ("quasistationary approximation").

But, then, for many problems in optothermodynamics, the problem of predetermining the shape of the radiation pulse is removed, which simplifies the experiments significantly.

Such problems, besides their intrinsic physical interest, are very important in applications. For example, they simulate the phenomena occurring in systems for pumping solid state lasers, in which the radiation sources are powerful pulsed lamps that are placed in a cooling liquid.[4,5] For this reason, we will consider these phenomena in somewhat greater detail.

As an example, let us examine the following one-dimensional problem.[6] Let an electromagnetic plane wave irradiate one of the faces of a rectangular cuvette, filled with a liquid (the Poynting vector of the wave is normal to the surface of the cuvette). The absorption coefficient of the liquid satisfies the condition $K\delta \gg 1$, where δ is the thickness of the liquid layer in the direction of propagation of the radiation.

The condition for the applicability of the quasistationary approximation now has the form $u\tau \gg \delta$. On the other hand, the upper limit to the duration of the laser pulse is determined by the inequality $\chi\tau K^2 \ll 1$, which allows us to neglect the effects of thermal conductivity.

The values of the pressure that can be attained in the liquid during the experiments, corresponding to the given problem, are limited by the strength of the cuvette and in actual cases do not exceed several hundred bar, which lies within the limits of the applicability of linear acoustics. For this reason, it is convenient to choose the pressure as one of the independent thermodynamic variables and to linearize the problem with respect to this variable.

However, in the more interesting case involving radiation intensities of any significance, when the liquid can make a transition into the supercritical state, it is not possible to choose a second independent variable, with respect to which the problem could be linearized. This is related to the fact that the part of the laser pulse energy that goes into increasing the pressure in the liquid is "spread out" throughout the entire volume, which leads to "physical averaging" of the pressure. This does not occur with any other variables. The profiles of temperature, density and so on remain "frozen" in the liquid and, even though their average values are small (the average change in density throughout the volume, in general, equals zero), the local variations can be very large in the range $Kx \lesssim 1$ (where x is the distance measured from the inner surface of the cuvette in the direction of propagation of radiation; this region will be referred to below as the core). And, since

most of the energy is liberated in the core, even small errors in the determination of thermodynamic variables in this region can lead to large distortions in the real situation. For this reason, the phenomenon can be described correctly only on the basis of a solution of a nonlinear hydrodynamic problem. Such a solution and its comparison with experiment will be presented briefly below.

Let us first make some remarks concerning the formulation of the problem. If the source of the radiation is a pulsed lamp, then due to its wide-band emission it is necessary to take into account the wavelength dependence of the absorption coefficient for radiation. However, it is possible to introduce some averaged absorption coefficient, which describes adequately the dissipation of radiation energy in the liquid.[5] In addition, the pulsed lamp is usually placed directly inside the cuvette, which alters the symmetry of the problem. However, if the condition $KR \gg 1$ is satisfied, where R is the external radius of the envelope of the lamp, which, as a rule, occurs under actual experimental conditions (see below), then the problem describing the absorption of radiation in the core is two-dimensional. So far as the liquid outside the core is concerned, as will be seen below, if the system has translational symmetry along the axis of the lamp (which makes the problem two-dimensional), the shape of the inner surface of the cuvette is generally unimportant.[1)]

It is convenient to choose the specific enthalpy w as an independent thermodynamic variable. Since we make use of the principle of corresponding states below, the variables entering into the formula for the enthalpy include the true enthalpy of the liquid, measured from absolute zero, and, as already mentioned, the pressure p. In this case, the equation of state of the liquid has the form $\rho = \rho(w, p)$. The coefficient of absorption for radiation in the liquid is determined by the state of the liquid, i.e. $K = K(w, p)$. With these assumptions, the equations of hydrodynamics have the following form:

$$\rho \frac{\partial w}{\partial t} - \frac{\partial p}{\partial t} = q(t) K \exp\left(-\int_0^x K\, dx'\right), \tag{2.1}$$

$$\frac{\partial p}{\partial x} = 0, \tag{2.2}$$

$$\rho = \rho(w, p), \tag{2.3}$$

$$K = K(w, p). \tag{2.4}$$

These equations must be supplemented by the initial conditions

$$p(0, x) = p_0, \quad w(0, x) = w_0 \tag{2.5}$$

and by the conservation of mass law

$$\int_0^\delta \rho\, dx = \rho_0 \delta = \text{const}. \tag{2.6}$$

Here, $q(t)$ denotes the intensity of the radiation incident on the liquid $[g(t) = 0$ at $t \leq 0]$.

[1)]Assuming that the minimum distance from the envelope of the lamp to the surface of the cuvette is large in comparison with K^{-1} (the walls of the cuvette do not enter into the core region).

In order to solve the problem, it is convenient to represent the quantity $w' \equiv w - w_0$ in the form $w' = w_1' + w_2'$, where the terms w_1 and w_2 satisfy the equations

$$\rho \frac{\partial w_1}{\partial t} = q(t) K \exp\left(-\int_0^x K\, dx'\right), \tag{2.7}$$

$$\rho \frac{\partial w_2}{\partial t} = \frac{\partial p}{\partial t}. \tag{2.8}$$

We thereby separate two essentially different mechanisms for heating the liquid: as a result of absorption of radiation and as a result of an increase in pressure. Estimates show that in the core region $w_1' \gg w_2'$, while in the remaining volume of the liquid the opposite inequality is satisfied.[5] Physically, this indicates that within the core the liquid absorbs nearly all the radiation, it is strongly heated and it expands, pressing like a piston against the remaining mass of the liquid, which is compressed adiabatically and as a result heats up.

It is clear from what has been said that the quantity w_1' can be neglected outside the core in comparison with w_2', while the problem (2.1)–(2.6) can be linearized with respect to all variables in view of the small adiabatic compressibility of real liquids. From here, we immediately find that $w_2' = p'/\rho_0$.

The equation of state of the liquid in the region of the core can be represented in the form

$$\rho(w, p) \approx \rho(w, p_0) + \left(\frac{\partial \rho}{\partial p}\right)_w p'. \tag{2.9}$$

As will be evident from what follows, p' is always inversely proportional to δ, while at the same time the other quantities on the right side of (2.9) depend weakly on δ. For this reason, for sufficiently large δ, the change in density within the core, caused by an increase in pressure, can be neglected in comparison with the change connected to the increase in enthalpy. Estimates show that the limits placed in this connection on the quantity δ, usually reduce to the same condition $K\delta \gg 1$. In addition, taking into account the fact that near the core $w_2' \ll w_1'$, we find that here the equation of state degenerates in to the equation of an isobar $\rho = \rho_p(w_1)$. From what has been said, it is clear that within the limits of applicability of the present analysis the actual value of p in the equation for the isobar is unimportant. For this reason, the subscript p will be deleted in what follows, $\rho_p(w_1) \equiv \rho(w_1)$. The same is true concerning K, i.e. $K \approx K(w_1)$.

In this case, Eq. (2.7) can be solved in general form with respect to w_1 for practically arbitrary functional dependences of ρ and K on w_1.

The method for solving such equations is presented in Ref. 7. Omitting the cumbersome computations, we immediately present the final result:

$$x = \int_{w_1}^{w_M} \rho(w) \left[K(w) \int_{w_0}^{w} \rho(w')\, dw\right]^{-1} dw, \tag{2.10}$$

where $w_M(t) \equiv w_1|_{x=0}$ is the maximum value of the enthalpy of the liquid, attained at the time t. The quantity w_M is most easily determined in the case of bulk absorption of radiation ($K = \mu\rho$, $\mu = \text{const}$). In this case [see (2.7)]

$$w'_M = \mu \int_0^t q(t')\,dt'. \tag{2.11}$$

Equation (2.10) determines the function $w_1 = w_1(x, t)$ in an implicit form.

It is convenient to represent changes in density in the form $\rho' = \rho'_1 + \rho'_2$, where ρ'_1 is connected to the direct heating by radiation (i.e. with w_1), while ρ'_2 is connected to the heating due to adiabatic compression ($\rho'_2 = p'(u_0^2)$. Using the law of conservation of mass (2.6) and taking into account the fact that according to (2.10)

$$\int_0^\delta \rho'_1(w_1)\,dx \approx \int_{w_M}^{w_0} \rho_1 \frac{dx}{dw_1}\,dw_1$$

we obtain for p' the expression

$$p' = \tilde{p} \int_{w_0}^{w_M} [\rho_0 - \rho(w)] \frac{\rho(w)}{\rho_0} \frac{K_0}{K(w)} \left[\int_{w_0}^{w} \rho(w')\,dw' \right]^{-1} dw, \tag{2.12}$$

where $\tilde{p} \equiv u_0^2\rho_0/\Lambda_0$ and $\Lambda_0 \equiv K_0\delta$ is the optical thickness of the unperturbed liquid.

Equations (2.9)–(2.12) together with the condition $\rho' = \rho_1(w_1) + (p'/u_0^2)$ represent a complete solution to the problem posed. Corrections to the solution, due to the influence of the increase in w_2 and p on the formation of the profile of thermodynamic variables near the core can, if necessary, be obtained by the method of successive approximations.

We emphasize that at $\rho'_1(\omega_1) < 0$, the liquid in the core expands, and furthermore, inasmuch as the volume of the core is small, in order that the conservation of mass law be satisfied, $|\rho'_1(w_M)| \gg p'/u_0^2$, i.e., the change in density in the core can be very large.

In this manner, in the case being examined, the liquid in the core region is comparatively easily transformed into a state with low density and high pressure and temperature. We emphasize that for a cuvette with a good airtight seal such states of the liquid are comparatively "long-lived." The time required for smoothening the density and temperature profiles is of the order of $(K^2\chi)^{-1}$, which in typical situations[4-6] constitutes 0.1 s and can be significantly increased, since the quantity K can vary over a wide range.

For the reasons indicated, such a method for acting on a liquid with radiation appears to the authors to be particularly useful for studying the physico-chemical properties of a liquid at values of p, ρ, and T that are difficult to attain.[6]

Let us again examine Eq. (2.12). For small energy deposition, when the linear approximation is also valid in the core region, (2.12) reduces to

$$p' \approx \Gamma_0 \frac{1}{\delta} \int_0^t q(t')\,dt', \tag{2.13}$$

where Γ_0 denotes the Grüneisen constant for the given liquid under the initial conditions ($\Gamma \equiv \alpha u^2/C_p^3$). The expression (2.13) has a simple physical meaning and can be immediately written down without any calculations. Indeed, $S\int_0^t q(t')dt'$ is the total change in the internal energy of the liquid (here, S is the surface area of a face of the cuvette through which the radiation is introduced), while Γ, by definition, is a dimensionless coefficient of proportionality between the volume internal energy density of the body and the pressure corresponding to it.[2)] From here, expression (2.13) follows immediately.

In the other limiting case of very large energy input, when $\rho(w_M) \ll \rho_0$, the following asymptotic value is obtained from Eq. (2.12) for the increase in pressure dp':

$$dp' \approx \Gamma_\infty \frac{1}{\delta} q(t)\,dt, \quad \Gamma_\infty \equiv u_0^2\rho_0 \left(\int_{w_0}^{\infty} \rho(w)\,dw \right)^{-1}. \tag{2.14}$$

$\int_{w_0}^{\infty} \rho dw$ converges for any arbitrarily weak attractive force, existing at large separation distances between molecules in the liquid, and has the physical meaning of a volume energy density, which the liquid acquires on condensation at constant pressure from an infinitely rarefied state to a state corresponding to an enthalpy density equal to w_0. But, then, in order of magnitude $\int_{w_0}^{\infty} \rho dw \sim u_0^2\rho_0$, i.e. the expressions (2.13) and (2.14) differ only by a renormalization of the Grüneisen constant, so that the function (2.12) can formally be rewritten in the form (2.13), introducing an effective Grüneisen constant $\Gamma(w_M)$. From the fact that Γ_∞ is of the same order of magnitude as Γ_0, it follows that $\Gamma(w_M)$ varies comparatively little.

Let us return to Eq. (2.12), which can be written in the form $p' = \tilde{p} f(w_M)$, where $f(w_M)$ is a dimensionless function of the enthalpy. We assume everywhere below that $K(w) = \mu\rho(w)$, $\mu = \text{const}$ (bulk absorption). Then, referring w to the critical value of the enthalpy w_C, within the limits of applicability of the principle of corresponding states, it may be expected that the function $f(w/w_C)$ will be a universal function that describes the response of various liquids to the action of radiation. Quantitative calculations, using real equations of state tabulated in Ref. 9 and 10, have shown that the function $f(w/w_C)$ for greatly different liquids (ethyl alcohol, benzene, ammonia, water) almost coincide within the error admitted by the method.

We emphasize that the initial conditions must also satisfy the principle of corresponding states (i.e., the ratios p_0/p_C and w_0/w_C must be the same for different liquids). Figure 2 illustrates the function $f(w_M/w_C)$ at $p_0/p_C = 0.015$ and $w_0/w_C = 0.37$, which corresponds to the normal conditions for ethyl alcohol. The values of Γ_0 and Γ_∞ in this case equal $\Gamma_0 \approx 0.6$ and $\Gamma_\infty = 1.6$.

Everything that has been stated above corresponds to the case for which there is no liquid-vapor transition as a result of the action of radiation. Let us determine when this will occur. Since $p = p(t)$, while $w = w(t, x)$, for each moment in time there corresponds a single value of p and a continuum of values for w, contained in the interval $p'/\rho_0 \leq w' \leq w'_M$. For this reason, the states of the liquid on the (w, p) surface will be represented by some two-dimensional region, bounded on the

[2)] Usually, for condensed media $\Gamma_0 \sim 1$.

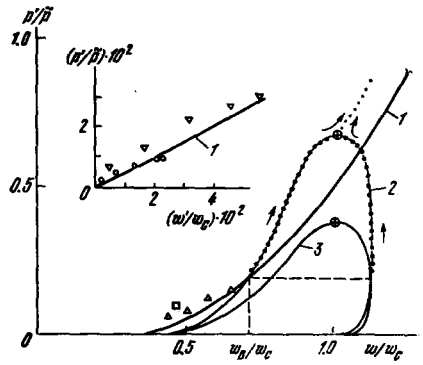

FIG. 2. (w, p) diagram for action of radiation on 96% ethyl alcohol. 1—universal function $f(w_M/w_C)$; the initial region of this curve is shown on a smaller scale in the upper left. 2—the binodal line for $\tilde{\pi} < \tilde{\pi}_K$ ($\tilde{\pi} \equiv \tilde{p}/p_C = 1.5$); the liquid boils for $w_M > w_B$. The further evolution of the heterogeneous phase mixture is shown with boldface dots; the arrows indicate the direction of motion of the dots with time; ⊗denotes a critical point. 3—the binodal line for $\tilde{\pi} > \pi_K$ ($\tilde{\pi} = 2.6$); boiling does not occur. The experimental data correspond to the pressure pulses illustrated in Fig. 3 (○—1, △—2, ▽—3, □—4); in the latter case, only the point for which $w_M < w_B$ is shown.

right by the curve $p = p(w_M)$, determined by Eq. (2.12), to the left by the straight line $p' = \rho_0 w'$, and above by the straight line $p = p_M$, corresponding to the maximum pressure attained in the liquid at the end of the laser pulse. Further, let the equation $p = p_B(w)$ describe the liquid-vapor phase equilibrium curve (binodal). Then, the liquid will not boil if one of the following conditions is satisfied: $w_M < w_B$, where w_B is the smallest root of the equation $p(w) = p_B(w)$ [here and below $p(w) \equiv p(w_M)$ and is determined by Eq. (2.12); see Fig. 2], or this equation has no solution in general. In the latter case, for sufficiently large inputs of energy, the liquid will be transformed into the supercritical state along a path completely lying within a single-phase region.

Since $f(w_M/w_C)$ is a universal function, the single parameter that determines the presence or absence of a solution to the equation $p(w) = p_B(w)$ is the quantity $\tilde{p}$ [see (2.12)]. With a variation in $\tilde{p}$ (for a given liquid, this in essence reduces to a variation in Λ_0) the curve $p(w)$ varies congruently. There exists a certain characteristic value $\tilde{p}_K$ at which it is tangent to the binodal. Since the equation of the binodal also approximately satisfies the principle of corresponding states,[11] the universal quantity will not be $\tilde{p}_K$, but $\tilde{\pi}_K = \tilde{p}_K/p_C$. For the curves shown in Fig. 2, $\pi_K \approx 2.1$. In the case of ethyl alcohol, this corresponds to an initial optical thickness $\Lambda_{0K} \sim 83$.

For $\tilde{p} < p_K$ and sufficiently large energy input ($w_M > w_B$), the liquid will boil.[3)] A rigorous analysis of the boiling process is impossible on the basis of the one-dimensional considerations presented above. However, it is physically evident that if the liberation of energy in the liquid will continue, then due to the fact that the total volume is enclosed, it will lead to an increase in pressure as before. In this case, the points that describe on the (w, p) diagram the state of the liquid and the vapor phase in the boiling layer will move along the two branches of the binodal curve ("liquid" and "vapor"; see Fig. 2) in the direction of the critical point. With further liberation of energy, this process must continue until the pressure in the liquid is equal to p_C. At this instant, the points that describe the state of the heterogeneous phase mixture, moving along both branches of the binodal curve, will coalesce at the critical point, i.e., the entire boiling region will move into the vicinity of the critical point. With further liberation of energy, the liquid will again heat up as a single-phase system.

In this manner, for any value of the optical thickness of the liquid layer in the cuvette that satisfies the inequality $\Lambda_0 > \Lambda_{0K}$ (where Λ_{0K} is a constant for the problem) and arbitrary initial conditions in the region $p_0 < p_C, \rho_0 > \rho_C$, with sufficiently large inputs of energy at some point in time there will necessarily exist a region in the liquid located in the vicinity of the critical point.

This assertion becomes completely obvious, if it is recalled that, as noted above, there exists a profile in the liquid at each fixed moment in time for values of the specific enthalpy, the magnitude of which falls into the interval $w_m(t) \leq w \leq w_M(t)$. Beginning at some instant the critical value of the enthalpy falls within this interval, so that a region arises in the liquid in which $w = w_C$. Inasmuch as the pressure is the same at all points in the cuvette, at the instant that $p(t)$ becomes equal to p_C, the indicated region is necessarily near the critical point. The condition $\Lambda_0 > \Lambda_{0K}$ guarantees that the pressure in the liquid does not exceed p_C before w_K falls into the interval $[w_m; w_M]$.

The moment at which the critical point is attained can be detected experimentally by the appearance of critical opalescence. By measuring the energy introduced into the liquid and the pressure at the instant critical opalescence appears, it is possible to determine two critical parameters (p_C and w_C) immediately. For this reason, the indicated method can be used for diagnostics of the critical point.[6,12] It is important that the pressure in the liquid can be determined directly by the indications of gauges placed in the liquid,[5,12] as well as by measuring the density outside the core ($p' = u_0^2 \rho'$), which in turn can be carried out by optical measurements with great precision. In other words, p_C and w_C can be determined without direct contact with the liquid during the experiment, which makes it possible to study corrosive and toxic liquids when necessary.

Another important advantage of the indicated method is the possibility of using small volumes of the liquid being studied for performing the measurements (actually, volumes ~1 cm³).

Let us proceed to a discussion of the experimental

[3)]For pulsed heating of a liquid, the liquid boils with a transition into a metastable state, which is the greater, the greater the rate of energy liberation. For this reason, boiling begins when w_M exceeds w_B, as suggested in the text. These problems will be examined in greater detail in Chapter 3 of the present review.

results. The appropriate experiments were performed in Ref. 5 and 12 for the purpose of simulating the operational conditions of powerful pumping sources for solid state lasers, which imposed great limitations on the experiments. The most important of these is a limitation on the maximum radiation energy density with a magnitude ~5 J/cm² (with $\tau \sim 500$ μs), which is attained by the maximum performance of the pulsed lamps used in Refs. 5 and 12 as radiation sources (a tubular pulsed Xe 400 lamp, ϕ 11×250). The lamp was placed coaxially inside a cylindrical steel chamber ($\delta = 7$ mm). The space inside the chamber was filled with the liquid being studied (96% aqueous solution of ethyl alcohol, in which a special dye was dissolved, which allowed varying its coefficient of absorption). In order to detect pressure pulses that arise in the liquid at the time the lamp is flashed, piezoelectric pressure gauges were used, calibrated according to the ruptured diaphragm method.[13] Typical oscillograms of the pressure pulses are shown in Fig. 3. This figure also shows the shape of the pulse of radiation, lying in the absorption band of the liquid (220–400 nm). The comparatively rapid relaxation of pressure after the lamp is flashed for large energy of input (curve 4) is explained by the inadequate airtight seal of the cuvette.

The results of the measurements of pressure pulses for different values of the absorption coefficient and energy input to the liquid are shown in Fig. 2 in terms of dimensionless variables. The good agreement between theory and experiment is evident. However, the available experimental data are insufficient for a complete description of the function $f(w_M/w_C)$: all the experimental points fall on the initial part of the corresponding curve.

The optothermodynamic method for diagnostics of the critical point was first attempted experimentally in Ref. 12. The experimental setup was the same as in Ref. 5, but the chamber in which the lamp was placed had an optical window that allowed recording the radiation scattered by the liquid. A 96% ethyl alcohol solution was again chosen as the liquid to be studied, which permitted a comparison of the measured values of the critical pressure with the tabulated data.

The characteristic radiation of the pulsed lamp scattered from a thin ($\sim K^{-1}$) layer of liquid adjacent to the surface of the lamp envelope was studied in the surface

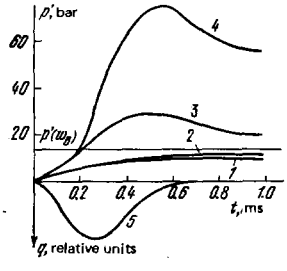

FIG. 3. Oscillograms of pressure pulses in an airtight cuvette (1–4) and the shape of the radiation pulse (5). $\Lambda_0 = 12$ (1, 3) and $\Lambda_0 = 180$ (2, 4); the total energy input constitutes 1.7 J/cm² (1, 2) and 4.7 J/cm² (3, 4). For $\Lambda_0 = 180$, the instant at which boiling appears corresponds to a pressure $p'(w_B) \approx 14$ bar[5].

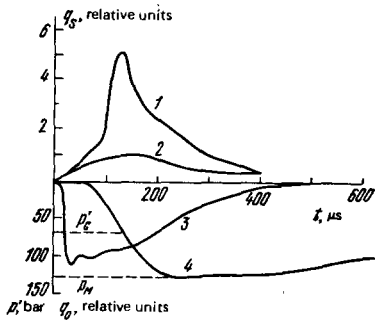

FIG. 4. The action of radiation on a 96% aqueous solution of ethyl alcohol. 1, 2—intensity of scattered radiation, 3—intensity of radiation from the lamp, 4—pressure pulse in the liquid with $p_M > p_C$, corresponding to the curve 1. For $p_M < p_C$, when the critical point is not attained, the peak in the scattered intensity is also absent (2)[12].

of the lamp envelope and in a direction perpendicular to the axis of the lamp. Typical results of the measurements are shown in Fig. 4. It is evident that the intensity of the scattered radiation for $\Lambda_0 > \Lambda_{0K}$ has a distinct maximum for $p \approx p_C$, the position of which in general does not coincide with the maximum in the intensity of the radiation emitted by the lamp. In addition, the effect has a threshold character: when the critical pressure is not attained in the liquid, the peak in the intensity of the scattered radiation is also absent.

In this manner, the data obtained in Ref. 12 indicate the efficacy of the optothermodynamic method for diagnostics of the critical point and for measuring the critical parameters of a substance.

3. THE LIQUID-VAPOR PHASE TRANSITION UNDER THE ACTION OF LASER RADIATION

In this chapter of the review, the modern understanding of the kinetics of boiling in a superheated liquid are briefly presented. In making this presentation, our purpose is not to describe any specific experiments, and the basic theoretical situation is presented in a very compressed manner, but with a detailed indication of the appropriate literature.

At the same time, we would like to emphasize that many problems in the kinetics of boiling (which will be described below) are clearly inadequately studied, especially from the experimental point of view. The action of laser radiation on the liquid being studied appears to us as a very convenient method for creating local superheating in the liquid, which has many advantages in comparison with the traditional methods (electric heating and so on). The main advantages are the possibility of introducing large energy fluxes into the liquid and the possibility (for small coefficients of absorption) of a comparatively uniform distribution of this energy throughout the volume of the liquid being studied.

The reasons indicated encouraged us to include the present section in this review.

a) Metastable liquid

Let us briefly recall some of the general principles of the thermodynamics of a metastable liquid.[3,11]

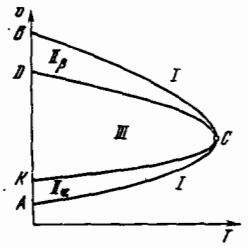

FIG. 5. Tv diagram of the states of a liquid (schematic). ACB-binodal, KCD-spinodal, C-critical point, I-stable region, II_α, II_β—metastable region.

For clarity, we shall make use of the Tv diagram, illustrated in Fig. 5. The region I is a thermodynamically stable single-phase region. The (binodal) curve ACB separates it from the metastable region II (II_α corresponds to the superheated liquid, II_β corresponds to the supercooled vapor). The curve ACB is a projection onto the Tv plane, the line of intersection of two surfaces representing the chemical potentials corresponding to the liquid μ_L and gaseous μ_V phases. For this reason, by definition, $\mu_L = \mu_V$ everywhere along the curve ACB. In the metastable region II_α, $\mu_V < \mu_L$, i.e. the gas (vapor) phase is thermodynamically more favorable than the liquid phase (in region $II_\beta \mu_V > \mu_L$, i.e., the liquid phase is more favorable in this region). However, since for the chemical potentials of each of the phases the binodal curve is not remarkable in any way, the liquid in region II_α (or the vapor in region II_β) remains stable relative to small heterogeneous phase fluctuations. This indicates that fluctuations less than some critical value are dissipated without causing an instability. The separation into two phases begins only when the fluctuations attain a critical magnitude. When such a critical fluctuation does not penetrate deeply into the metastable region, it appears as a nucleus for a new phase (a gas bubble or liquid drop) with a thin transition layer between the two phases, which permits introduction of a physically sensible boundary separating the phases and a corresponding surface tension σ. For definiteness, let us examine further the region II_α. The minimum work for the formation of a gas bubble with radius r equals[4)]

$$R_{\min} = -(\mu_L - \mu_V) \cdot \frac{4}{3}\pi r^3 n + 4\pi r^2 \sigma, \tag{3.1}$$

where n is the number of particles per unit volume of the gas phase.

For a fixed state of the liquid, the work $R_{\min}$ depends only on the radius of the bubble r. The radius of the critical bubble r_K corresponds to the maximum of the expression (3.1).

For a stationary boiling process, the state of spontaneous formation of nuclei J ("nucleation rate") in this case equals

$$J = n_0 B e^{-R_{\min}/T}, \tag{3.2}$$

where n_0 is the number of particles per unit volume of the metastable phase. The factor B has the dimensions of $\sec^{-1}$. There exist various methods for roughly estimating this factor.[11] In order to determine the quantity B correctly, the solution of a kinetic equation that describes the boiling process is required. Apparently, this was done most consistently in Ref. 14, but the expressions obtained therein are very cumbersome and will not be presented here. Typical values for dielectric liquids are $B \sim 10^{-10}\ \mathrm{s}^{-1}$.

If the system in region I is abruptly transformed into region II_α at $t = 0$, then a characteristic time τ_S is required in order to establish stationary boiling. The transition of the boiling process into a stationary state was first discussed in the classical work of Ya.B. Zel'dovich,[15] who obtained the following expression for the nucleation rate:

$$J' = J e^{-\tau_S/t}, \tag{3.3}$$

where J is determined by Eq. (3.2). In subsequent studies,[16-19] it was shown that Eq. (3.3) gives a correct quantitative description of the temporal evolution of the boiling process. More rigorous estimates of the characteristic time τ_S are made in Ref. 18 and 19. In accordance with Ref. 18 τ_S is given by

$$\tau_S = 2\pi \left[\left(\frac{\partial^2 N}{\partial r\, \partial t} \right)_K \left(\frac{\partial r}{\partial N} \right)_K \right]^{-1}, \tag{3.4}$$

where N is the number of particles in the gas phase, located in the gas bubble with dimensions r. The index K denotes that the expressions entering into (3.4) are to be considered for the case of a bubble with critical size. A similar expression was also obtained in Ref. 19. Estimates using Eq. (3.4) give a value $\tau_S \sim 10^{-9} - 10^{-8}$ s for dielectric liquids[11]; for molten metals τ_S is significantly lower ($10^{-13} - 10^{-11}$ s[20]). As evident from Eq. (3.3), if the time for heating the liquid is small compared to τ_S, then the boiling process does not have time to "adjust itself" to changes in the degree of overheating, which leads to a deeper penetration into the metastable region than with slow "adiabatic" heating of the liquid.

We note that the characteristic time for boiling, generally speaking, is not related to τ_S and depends on the formulation of the problem. For example, it can be defined either as the average time required for the appearance of at least a single bubble of critical size somewhere in the volume of liquid being studied or as the time over which the total volume of the vapor phase becomes commensurate with the volume of the liquid[5)] and so on.

The difference $\mu_L - \mu_V$ increases in proportion to the penetration into the region II_α, which leads to a decrease in r_K [see (3.1)], so that finally a macroscopic

[4)]Using the thermodynamic identities, the expression for $R_{\min}$ can be written in various other equivalent forms[3,11].

[5)]In this case, assuming the discussion does not concern the crudest estimates, it is necessary to take into account the fact that energy is expended on the formation of bubbles, and for this reason, the degree of overheating of the liquid decreases in proportion to the increase in the number and dimensions of bubbles, which, in its turn, alters the kinetics of the phase transition. A correct solution of such a self-consistent problem was first given in Ref. 21 for the case of condensation precipitation from a supersaturated solution.

treatment becomes impossible.

The metastable region *II* is separated from the region with absolute thermodynamic instability (the region of lability) *III* by the curve *KCD* (spinodal). Both curves *ACB* and *KCD* coalesce at the critical point *C*. The isodynamic stability coefficients vanish along the spinodal, i.e.,

$$\left(\frac{\partial T}{\partial S}\right)_p \equiv \frac{T}{C_p} = 0, \quad -\left(\frac{\partial p}{\partial v}\right)_T \equiv v\beta_T = 0,$$

so that in region *III* C_p and β_T are negative.

Let us examine the details of phase transitions in a metastable liquid (region II_a) near the lability boundary.

The nucleation rate in this case is determined according to Eq. (3.2) as before (but, of course, with a different value for the factor B), but the expression for $R_{\min}$ cannot now be represented in the form (3.1). It turns out[22] that critical fluctuation near the spinodal curve has nothing in common with the nuclei of a new phase, but rather represents a smooth change in the density of the liquid, which nevertheless is everywhere greater than the equilibrium density of the gas phase ρ_V. The characteristic size of the region is greater the closer we approach the spinodal curve, while on the spinodal curve itself it becomes infinite. On the whole, a phase transition near the lability boundary proceeds as shown schematically in Fig. 6. In this manner, the problem concerning the magnitude of the surface tension near the spinodal, first states by Gibbs,[23] is removed, at least for a critical fluctuation, since the boundary separating the phases is simply absent.

The lability region *III* is a region in which arbitrarily small perturbations of a single-phase system have a tendency toward unlimited growth, which finally leads to a separation of the system into two phases.

The kinetics of a phase transition in the region of absolute instability were first discussed by Zel'dovich and Todes.[24] However, this work was performed before the development of the fluctuation theory of the critical point (see, for example, Ref. 25) and for this reason needs to be made more precise.

We note that the application of the methods of the fluctuation theory of critical phenomena to the study of metastable states, in its turn, requires additional corroboration due to the finite lifetime of such states,

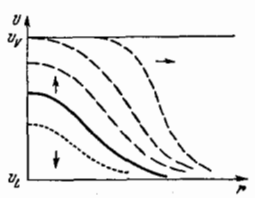

FIG. 6. A phase transition near the lability boundary (schematic). v_V and v_L denote the specific volume of the stable gas and metastable liquid phases, respectively. The boldface line represents the critical fluctuation. The arrows indicate the direction in which the fluctuations develop. Subcritical fluctuations dissipate, which supercritical fluctuations grow until the density in the center of the fluctuation attains $\rho_V \equiv v_V^{-1}$; after this, the fluctuation "spreads out".

while it is necessary to find the settling time in order to determine the scaling properties. This time increases without limit as the singular point (in this case, the spinodal curve) is approached. However, these problems have not been studied in detail as far as we know.

In concluding this section, we note once again that due to the recent progress in the techniques of laser experiments, most of the problems discussed here pass from abstract discussions to experimentally observable effects. In particular, it would be possible to obtain a great deal of information by studying the scattering of light on large scale density fluctuations near the lability boundary, by studying experimentally the kinetics of a phase transition in the region of absolute instability, and so on. However, as far as we know, no experiment of this type has yet been performed.[6)]

It should be especially noted that, in using lasers to create metastable states, it is necessary to focus the radiation inside the volume of the liquid being studied. When the radiation acts on the free surface, the creation of metastable states is inhibited by the appearance, in this case, of an instability in the vaporization front, with which the following section is concerned.

b) Instability of the vaporiation front

The experimentally observed laws governing the vaporization of condensed substances as a result of the action of laser radiation can be satisfactorily explained by starting with the model of surface vaporization (see, for example, Ref. 32). In accordance with this model, vaporization occurs from a thin (of the order of interatomic distances) surface layer of a condensed phase, to which energy is transferred by thermal conductivity from the region in which light is absorbed. Since the depth to which light penetrates inside the condensed phase, even for the most strongly absorbing substances (metals), is large in comparison with the thickness of the layer from which vaporization occurs, the temperature profile inside the evaporating body has a maximum.

It is easy to see that in this case the planar phase-separation boundary can turn out to be unstable with respect to small perturbations in its shape.[127] Indeed, when some part of the boundary is displaced toward the hotter condensed phase, the flow of heat to this region increases, which leads to further acceleration of the boundary. In this manner, the physical nature of the instability being examined consists in the fact that the vaporization front moves in the same direction as the temperature gradient. For this reason, it is apparent that the amplitude of the increasing perturba-

[6)]Interesting results concerning the spinodal properties of binary liquid mixtures, solid solutions, and alloys are contained in Ref. 26–28. We also draw attention to a recent review[125], which is concerned with the spinodal separation of different thermodynamic systems and which contains an extensive list of references. However, inasmuch as most of the problems examined in the cited references lie outside the framework of the present review, it is not possible to examine the work presented therein in detail.

tions is limited in this case by the thickness of the surface layer, in which the flow of heat is directed from the condensed phase to the vaporization front, i.e., the distance at which the temperature maximum occurs.

This description of the development of the process assumes that bulk boiling does not occur. Section C of this chapter will be devoted to this problem. It is significant, however, that bulk vaporization in fact leads to the same result as the thermal instability being studied, viz., to the destruction of the overheated layer and dispersing of the condensed phase. In this manner, the appearance of metastable states in experiments involving laser vaporization is unlikely and there is no sense in discussing this problem.

Let us briefly consider the quantitative description of the instability mentioned. The temperature distribution established in the condensed phase satisfies the equation

$$C\rho \frac{\partial T}{\partial t} = \varkappa \Delta T + Q, \quad x \geqslant 0,$$
$$Q = Aq_0(t) K \exp\{-K[x - X(y, t)]\}, \tag{3.5}$$

where $X(y,t)$ is the coordinate of the phase separation boundary. For simplicity, we neglect the temperature dependence of the optical and thermophysical properties of the substance. In addition, we assume that $q_0(t)$ varies little over the time $\sim \chi/V_0^2$, where V_0 is the speed of the vaporization front in the quasistationary regime.

Equation (3.5) must be supplemented by boundary conditions. We will choose the boundary condition for $x \to \infty$ in the form $T_{x \to \infty} 0$. The other two conditions are given on the boundary $x = X(y,t)$. One of these relates the normal (with respect to the perturbed boundary) component of the temperature gradient in the condensed phase to the energy expended on vaporization. If the perturbation has a small curvature, this condition can be written approximately in the form[7)]

$$\varkappa \frac{\partial T}{\partial x} = \lambda \rho \dot{X} \quad \text{for} \quad x = X(y, t), \tag{3.6}$$

where the dot indicates a derivative with respect to time.

The second boundary condition determines the dependence of the speed of the vaporization front on the temperature of the surface of the condensed phase and follows from the equation describing the kinetics of vaporization. In experiments involving laser vaporization, the vapor pressure on the surface usually significantly exceeds the pressure of the surrounding atmosphere, and for this reason, it can be assumed that the vaporization occurs in a vacuum. In this case, the mass flow and the speed of the vaporization front are proportional to the saturated vapor pressure, (see, for example Ref. 32, as well as Chapter 5 of this review). Taking into account the effect of the finite curvature of the evaporating surface on the magnitude of the pressure of the saturating vapor above it,[3] the expression for the rate of vaporization takes the form

$$\dot{X} = U \exp\left\{-\frac{1}{T(X, y, t)}\left[\lambda_1 + \frac{\sigma}{n_0}\left(\frac{1}{R_1} + \frac{1}{R_2}\right)\right]\right\}, \tag{3.7}$$

where U and λ_1 are constants, equal in order of magnitude to the speed of sound in the condensed phase and the microscopic heat of vaporization, respectively (we neglect here the weak temperature dependence of U, which is not important for the following analysis), the exact values of which are obtained from a comparison with the experimental data on the saturating vapor pressure; $R_{1,2}$ are the values of the main radii of curvature of the evaporating surface (the normal is directed into the gas phase).

Equation (3.7) is valid for $T \ll \lambda_1$. It will be assumed everywhere below that this inequality is satisfied. We note also that if Eq. (3.7) is formally generalized to interatomic distances, then for $R_{1,2} \sim n_0^{-1/3}$ all the terms in the exponential are of the same order of magnitude. From here follows the effective relationship between λ_1 and σ: $\lambda_1 \sim \sigma n_0^{-2/3}$.

The problem (3.5)–(3.7) has a quasistationary solution in the form of a plane vaporization wave, propagating with a constant speed V_0. Let us introduce an "instantaneous" variable $\xi = x - V_0 t$. The solution to the quasistationary problem $T_0(\xi)$ is not difficult to obtain in an explicit form. However, below, we only need the values V_0, $T_0(0)$, and the derivative $T_{0\xi}(0)$, which can be obtained from the following simple considerations. Let us use the law of conservation of energy, which is obtained from (3.5) by integration with respect to ξ and has the form

$$\rho V_0 (\lambda + C T_0(0)) = A q_0.$$

Neglecting $CT_0(0)$ in comparison with λ and using (3.7), we then obtain

$$V_0 \approx \frac{Aq_0}{\lambda\rho}, \quad T_0(0) \approx \lambda_1 \left(\ln \frac{\rho \lambda U}{A q_0}\right)^{-1}.$$

The value of $T_{0\xi}(0)$ is determined from V_0 and the boundary condition (3.6).

Let us now examine the stability of the stationary solution with respect to small perturbations of the temperature distribution and the shape of the phase separation boundary in the form

$$T = T_0(\xi) + T_1(\xi) \exp(iky + \gamma t),$$
$$X = V_0 t + X_1 \exp(iky + \gamma t). \tag{3.8}$$

Here, $(1/R_1 + 1/R_2) \approx -X_{yy}$, while the boundary conditions imposed on the perturbed boundary $\xi = X_1 \exp(iky + \gamma t)$, must be transferred to the plane $\xi = 0$, expanding all the functions entering into them in a series in powers of X_1. The stability problem is then solved in the standard manner.

The analysis of the resulting dispersion relationship, performed in Ref. 127, shows that for the unstable branch of the spectrum $\gamma(k) = 0$ at $k = 0$ and is negative for small positive values of k, i.e., the problem is stable with respect to long wavelength perturbations. However, besides the trivial solution $k_1 = 0$, the equation $\gamma(k) = 0$ usually has two other real roots k_2 and k_3. In this case, in the region $k_2 < k < k_3$ the increment $\gamma(k)$ is positive, i.e., perturbations with such

---

7)A more precise condition, which takes into account the temperature jump in the Knudsen layer and the kinetic energy of the vapor, is used in Ref. 127.

wave numbers lead to the development of an instability. Finally, at $k > k_3$ the quantity $\gamma(k)$ is negative, so that the short wavelength perturbations also do not lead to the appearance of an instability. However, the reasons for stabilization of the instability in the long wavelength and short wavelength regions are very different.

The suppression of instability in the long wavelength region is explained by the fact that the dominant role in improving the conditions for heat transfer near the "indented" region of the surface is played by the heat flow "from the sides," i.e., in a tangential direction with respect to the unperturbed surface. When the curvature of the perturbed region is small, the tangential component of the heat flux is also small, so that the improvement in the conditions for heat transfer turns out to be insufficient to compensate for the heat losses related to the increase in the vaporization rate, and such perturbations are extinguished.

In the short wavelength region, the perturbation is stabilized by the presence of surface energy on the phase separation boundary and is explained by the fact that for a large curvature in the perturbed phase boundary the increase in the vaporization rate, related to improved conditions for heat transfer, is compensated by a decrease in this rate due to the drop in the pressure of the saturating vapor above the indented surface.

In the region of instability ($k_2 < k < k_3$) the quantity $\gamma(k)$ at first increases monotonically with an increase in k, reaching a maximum for some value $k = k_{max}$, and then, with further increase in k, it begins to decrease monotonically.

Analysis shows[127] that the quantity k_2 is always of the same order of magnitude as K. However, the values of k_{max} and k_3 significantly depend on the parameters of the problem. In general, these quantities are obtained from a numerical analysis of the dispersion equation. The analytical expressions are cumbersome and are not very accurate. However, in the physically important and interesting case, when the quantities k_2, k_{max}, and k_3 satisfy the conditions $k_2 \ll k_{max} \ll k_3$, a complete analytical analysis of the problem is possible. In this case

$$k_{max} \approx \left(\frac{Aq_0 n_0 K}{2\sigma\varkappa}\frac{\lambda_1}{T_0(0)}\right)^{1/3} \approx \left(\frac{Aq_0 K}{2C_A\sigma\chi}\ln\frac{n_0\lambda_1 U}{Aq_0}\right)^{1/3}, \tag{3.9}$$

$$k_3 \approx \left(\frac{n_0\lambda_1}{\sigma}\frac{T_{0\xi}(0)}{T_0(0)}\right)^{1/2} \approx \left(\frac{2k_{max}^3}{K}\right)^{1/2}, \tag{3.10}$$

where $C_A = C\rho/n_0$ is the atomic heat capacity (i.e., a number, since the temperature is measured in energy units).

The quantity $\gamma_{max} \equiv \gamma(k_{max})$ for $k_{max} \gg k_2 \sim K$ can be found directly from Eq. (3.7). The contribution of the perturbation in the temperature distribution to the dispersion equation, in this case, is small in comparison with the contribution from the perturbation in the shape of the vaporization front (the small parameter is K/k). For this reason, it can be assumed in (3.7) that $T(X, y, t) \approx T_0(X, y, t)$. Substituting here the expression (3.8) for X and neglecting the quantity $\sigma k_{max}^2/n_0$ in comparison with $\lambda_1 T_{0\xi}(0)/T_0(0)$, as a result

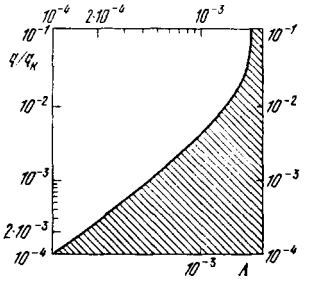

FIG. 7. The boundary for stability of a plane vaporization front. The stable region is shaded.

of the condition $k_{max} \ll k_3$, we obtain from (3.7)

$$\gamma_{max} \approx V_0 \frac{\lambda_1}{T_0^2(0)} T_{0\xi}(0). \tag{3.11}$$

The relationship between the instability of the phase boundary and the direction of the temperature gradient in its vicinity, as noted above, is immediately evident from the expression (3.11).

Using the condition (3.6), the expression (3.11) can be rewritten in the form

$$\gamma_{max} \approx \frac{V_0^2}{\chi C_A}\left(\frac{\lambda_1}{T_0(0)}\right)^2. \tag{3.12}$$

Since the time for establishing the quasistationary vaporization regime is of the order of χ/V_0^2,[32] it is evident from (3.12) that, in this case, the instability develops significantly earlier than the establishment of the quasistationary vaporization regime.

We note that expressions (3.9) and (3.12) can also be used with weakly nonstationary vaporization, if V_0 and T_0 are viewed as slowly varying functions of time (on a time scale much greater than γ_{max}^{-1}).

It is evident from Eqs. (3.9)–(3.12) that the magnitudes of k_{max}, k_3, and γ_{max} also decrease with a drop in the intensity of the laser radiation, i.e., the region in which the instability exists decreases (we recall that the lower boundary of the unstable region k_2 depends weakly on the parameters of the problem), as well as the maximum value of the increment. For some, sufficiently small values of k_0 the region in which the instability exists completely disappears, i.e., stable motion of the plane vaporization wave becomes possible. The threshold for the appearance of instability q^*, normalized relative to the quantity $q_K \equiv U\rho\lambda/A$, depends on the single dimensionless parameter $\Lambda \equiv K\sigma/(\lambda_1 n_0) \sim K n_0^{-1/3}$. The corresponding curve is shown in Fig. 7. It is evident from the graph that the region of stability has a real physical meaning only with the action of radiation on a metallic target. In this case, the characteristic value of q^* is of the order of $10^6 - 10^8$ W/cm^2. In the case of dielectric liquids, the maximum value of q^* does not exceed $10^2 - 10^3$ W/cm^2, while its typical value is much less than this magnitude.[8)] Such low intensities, as a rule, are not physically interesting, so that it may be asserted that when laser radiation is incident on the

[8)]The magnitude of q^* for dielectric liquids varies over a wide range, mainly due to the large variation in their coefficients of absorption. Values of q^* of the order of 10^2–10^3 W/cm^2 correspond to $K \sim 10^3$ cm^{-1}, the maximum value of K encountered at laser frequencies for pure liquids.

free surface of a dielectric liquid the plane vaporization front is always unstable. The development of the vaporization process in this case is determined by the nonlinear stage of the indicated instability and requires a separate examination.

We emphasize that the type of instability studied in Ref. 127 has a very general character. The results presented above are easily generalized to the case of a nonplanar phase separation boundary (interaction with aerosols), the case of sublimation of solids, and other types of phase transitions.

A distortion in the shape of the phase-transition front can lead to the excitation of capillary (in liquids) or Rayleigh (in solids) waves. Without changing the qualitative nature of the instability, such waves must lead to temporal modulation of the reflection coefficient for radiation and to other experimentally observable effects. This class of problems is interesting in itself and was not considered in Ref. 127.

In experiments concerning laser vaporization of condensed substances, many characteristic phenomena have been established that could be related to the thermal instability of the phase separation boundary. Thus, for example, it has been observed repeatedly that there is a sharp change in the nature of the light scattered from a metallic surface and in the magnitude of its reflectivity with the onset of intense vaporization, and that a significant part of the products in the laser destruction of metals consists of a liquid phase, while the average specific energy for destruction is always lower than the specific heat of vaporization (see, for example, Ref. 32). All of these phenomena can indirectly indicate the development of a thermal instability and the dispersing of the liquid phase related to it. The instability in the vaporization front under the action of laser radiation on the free surface of dielectric liquids (acetone, ethyl alcohol) observed in Ref. 33 and explained therein as an explosive decomposition of the metastable phase, in our opinion, should be explained not by this reason, but rather by thermal instability. We emphasize, however, that direct experiments, in which the thermal instability of the front of the phase transition is directly studied, have not been carried out and, from the experimental point of view, this problem remains open.

c) Volume and surface formation of vapor

The question concerning the relative contribution of volume and surface formation of vapor as a result of the action of laser radiation on the free surface of an absorbing liquid is apparently one of the most confused questions in the entire subject of this review. So far as we know, the first discussion of this problem appeared in Ref. 29.[9)] The authors of the cited work, beginning with the theory of homogeneous nucleation,[3,15] estimated the total surface area of the vapor bubbles located in the entire heated layer of liquid relative to the surface area of the free surface of this liquid. It was assumed that the criterion for comparing volume and surface mechanisms for vapor formation should be the commensurability of the corresponding surface areas. It followed from the results in Ref. 29 that in the case of a metallic target volume vapor formation can be neglected up to temperatures that are close to critical. However, the cited reference contained many inaccuracies, while the estimates made in it were based on approximations which were too crude. A more systematic analysis, taking into account the real temperature distribution in the liquid and the presence of impurities as well as bubbles of dissolved gases in the liquid, which are centers for vapor formation,[30] showed that there is a critical value for the intensity of laser radiation q_B, at which the volume process for vapor formation predominates. Unfortunately, the formulation of the problem adopted in Ref. 30 also turned out to be imprecise, which led to a significant decrease in the magnitude of q_B.

The problem concerning the role of volume boiling was studied most rigorously in Ref. 129. In this work, a temperature profile was obtained that corresponded to a plane stationary vaporization wave with a free liquid surface, taking into account the energy expended on melting (metals), the temperature jump in the Knudsen layer, and the loss of energy related to the vapor expansion. The effects due to volume vapor formation were examined as a perturbation supported on the motion of such a wave. The criterion for the transition to volume vaporization was the commensurability in the perturbation with the corresponding unperturbed quantities. In this case, inasmuch as the process of vaporization from the free surface is self-consistently related to the gas dynamic vapor expansion,[32] while the evaporation in bubbles is related to the dynamics of bubble growth, i.e., with a completely different phenomena, it is clear that the commensurability of the total surface area of bubbles, located throughout the overheated liquid, with the free surface area cannot be such a criterion. It is more natural to compare the mass flow, evaporated from the free surface, and the energy expended on evaporation from the free surface with the energy expended on the formation and growth of bubbles, and so on.

Of all such criteria, the one chosen should give the smallest value of q_B. Such a criterion will determine the transition to volume vapor formation. It was shown in Ref. 129 that such a criterion is the commensurability of the average distance between bubbles with the average dimensions of the bubbles. In this case, on the one hand, the bubbles that enter the free surface of the liquid at each instant will significantly perturb this surface, since the total surface area of such bubbles becomes commensurate with the surface area of the free surface. On the other hand, the total volume of the vapor concentrated in the bubbles becomes commensurate with the volume taken up by the overheated liquid phase, which must significantly alter the

[9)]We should also mention Ref. 31, in which the growth of vapor bubbles and the role of artificial centers for vapor formation in the liquid phase under the action of laser radiation on a metal were studied theoretically and Ref. 128, in which the force acting on a growing vapor bubble due to the recoil of evaporating molecules, caused by the unsymmetrical evaporation in the presence of a temperature gradient, was calculated.

average values of the thermophysical constants of the liquid near the boiling point. Both circumstances must lead to a significant distortion in the temperature distribution, calculated without taking the volume vapor formation into account, i.e., the volume boiling ceases to be a small perturbation superposed on the surface evaporation.

However, the quantity q_B, computed in Ref. 129, is greater, as a rule, than the threshold for the appearance of the thermal instability described in the previous section. For this reason, the unperturbed motion is not the plane wave of surface vaporization, but the regime that forms at the nonlinear stage in the development of the indicated instability. This changes the entire formulation of the problem, so that the question concerning the role of volume vapor formation due to the action of laser radiation on a free surface of an absorbing liquid, in essence, remains open.

4. OPTOACOUSTICAL PHENOMENA IN AN ABSORBING LIQUID

In concluding our treatment of the interaction of high power radiation fluxes with dielectric liquids, let us consider the various optoacoustical phenomena, i.e., the problems related to the generation of sound due to absorption of laser radiation in the liquid. Essentially new and interesting results, both theoretical and experimental, have been obtained in recent times. In this chapter we will discuss some of them. In doing so, without attempting to "grasp the infinite," we shall choose only those aspects of the problem that in our opinion have general interest and that exhibit the physics of the phenomenon.

a) Thermal and striction mechanisms for sound excitation

Optoacoustic effects in liquids, as in any other isotropic medium, can arise as a result of two physical mechanisms[10]: striction ("striction mechanism") and heating of the medium, accompanied by the appearance of thermal stresses ("thermal mechanism"). The striction mechanism allows optical excitation of sound in both transparent and absorbing media and, in this respect, it is more general than the thermal mechanism. However, it should be kept in mind that the absorbing properties of a medium, generally speaking, depend on the intensity of the optical radiation, and for this reason, it may be assumed that the thermal mechanism for optical excitation of sound is also effective for all media assuming that the exciting radiation is intense enough. An example of the thermal optical excitation of sound in a "transparent" medium is the optical (laser) breakdown of a medium, accompanied by the excitation of shock waves and acoustic waves in the medium.

In this review, we shall examine in detail only the thermal mechanism for optical excitation of sound in a liquid. As far as the striction mechanism is concerned, this mechanism, as will be shown below, plays a secondary role in absorbing liquids, with the exception of cases involving the generation of low-frequency sound and hypersound, when striction can become the dominant mechanism.

Evidently, it makes sense to compare the efficiency of the striction mechanism with the efficiency of the "linear" thermal mechanism. The latter mechanism involves the case when, as a result of heating the liquid due to the absorption of radiation, there is no change in the aggregate state (boiling, ionization, and so on) and the absorption properties of the liquid (as all the thermophysical parameters); if they do change in the irradiation process, then they change insignificantly (only as a result of a change in temperature and pressure in the absorption region).[11]

In order to compare the efficiency of the two optical methods for exciting sound, we first obtain the equation that the sound pressure must satisfy in the presence of both mechanisms. The starting point is the system of linearized equations of hydrodynamics, supplemented by the equations of state and heat transfer in the liquid:

$$\left.\begin{aligned}
&\rho\frac{\partial v}{\partial t}=-\nabla p'+\eta\Delta\mathbf{v}+\left(\zeta+\frac{\eta}{3}\right)\nabla(\nabla,\mathbf{v})+\frac{\rho}{8\pi}\left(\frac{\partial\varepsilon}{\partial\rho}\right)_T\nabla\langle\mathbf{E}^2\rangle,\\
&\frac{\partial\rho'}{\partial t}=-\rho(\nabla,\mathbf{v}),\\
&\rho T\frac{\partial s'}{\partial t}=\varkappa\Delta T'+Q,\\
&p'=\left(\frac{\partial p}{\partial\rho}\right)_s\rho'+\left(\frac{\partial p}{\partial s}\right)_v s'\equiv u^2\rho'+\frac{\alpha u^2\rho T}{C_p}s',\\
&s'=\left(\frac{\partial s}{\partial T}\right)_p T'+\left(\frac{\partial s}{\partial p}\right)_T p'\equiv\frac{C_p}{T}T'-\frac{\alpha}{\rho}p'.
\end{aligned}\right\}\qquad(4.1)$$

Here, the index 0 is omitted for brevity, in denoting the equilibrium values of thermodynamic variables; s is the specific entropy of the liquid; $\mathbf{v}$ is the velocity of the liquid; η and ζ are the coefficients of shear and bulk viscosity; ε is the dielectric permeability of the liquid; $\mathbf{E}$ is the electric field intensity of the optical radiation in the liquid (the brackets $\langle\cdots\rangle$ denote an average with respect to a period of the optical oscillations); Q is the density of heat sources, due to the absorption of optical energy in the liquid, given by $Q\equiv-(\nabla,\mathbf{S})$, where $S\equiv(c/4\pi)\langle(\mathbf{E},\mathbf{H})\rangle$ is the flux density for optical energy (Poynting vector). On the basis of the system (4.1) it is easy to obtain the equation

$$\Delta p'-\frac{1}{u^2}\frac{\partial^2 p'}{\partial t^2}+2\Xi\Delta\frac{\partial p'}{\partial t}=\frac{\alpha\rho T}{C_p}\left[\frac{(4/3)\eta+\zeta}{\rho}-\chi\right]\Delta\frac{\partial s'}{\partial t}-\frac{\alpha}{C_p}\frac{\partial Q}{\partial t}+\frac{1}{8\pi}\left(\rho\frac{\partial\varepsilon}{\partial\rho}\right)_T\Delta\langle\mathbf{E}^2\rangle,\qquad(4.2)$$

[10]When radiation is focused on the free surface of a liquid[34,35] or on the boundary separating two liquids with significantly different coefficients of absorption for radiation[36], a third, vaporization mechanism, arises due to the recoil action of vapors. This mechanism will not be discussed here. Some effects due to the action of the recoil pressure of vapors on molten metals will be examined below in Chapters 5 and 6.

[11]In the absence of resonant absorption, when the absorption coefficient can be represented in the form $K=\mu\rho$ (μ is a constant), the relative change in K, resulting from a change in temperature T' and pressure p', is given by $(K'/K)=-\alpha T'+\beta_T p'$. Taking into account the fact that for a liquid, $|\alpha|\lesssim10^{-3}$ deg^{-1}, $\beta\lesssim10^{-4}$ bar^{-1}, we obtain the result over a wide range in variation of T' and p' that $|K'/K|\ll1$. For more details see Chapter 2 of this review.

where

$$\Xi \equiv \frac{1}{2u^2}\left[\left(\frac{4}{3}\eta+\zeta\right)\frac{1}{\rho}+\chi\left(\frac{C_p}{C_v}-1\right)\right].$$

Far away from the region in which there exists an electromagnetic field ($E=0$), the thermal and striction pressure forces are absent, while the process for propagation of sound is isentropic. For this reason, in this region, the right side of Eq. (4.2) is equal to zero. In the region where there are sources of pressure ($E \neq 0$), thermal conductivity and viscosity can usually be neglected (if liquid metals and very viscous liquids are not considered), which is equivalent to neglecting the first term on the right side of Eq. (4.2). The quantitative condition for this is as follows:

$$\tau \ll \{l_{\min}^2/\chi,\quad l_{\min}^2/\nu\}, \tag{4.3}$$

where $\nu \equiv \eta/\rho$ is the kinematic viscosity, τ is the characteristic time for a variation of the power in the optical excitation (in the optical generation of sound pulses, when the power of the pulsed laser radiation is not modulated, τ is the duration of the laser pulse; in generating monochromatic sound with a frequency Ω, when the power of quasicontinuous laser radiation must be modulated at the same frequency Ω, the time $\tau \sim \Omega^{-1}$); $l_{\min}$ is the minimum size of the region for absorbing the exciting radiation. When the conditions (4.3) are satisfied, the heat transfer term $\varkappa \Delta T'$ in the last equation of the system (4.1) has no significance, so that $\rho T(\partial S'/\partial t) \approx Q(t)$, while the first term on the right side of (4.2) is actually smaller than the second term.

In this manner, when the conditions (4.3) are satisfied, the first term can be neglected in the entire region for generation ($E \neq 0$) and propagation ($E=0$) of sound. The condition (4.3) for nonmetallic and not very viscous liquids is often easily satisfied. The greatest limitations on the magnitude of τ occurs in strongly absorbing liquids, for which usually $l_{\min} \sim K^{-1}$. Thus, for CO_2 laser radiation ($\lambda = 10.6\ \mu$m), water, for example, has an absorption coefficient $K = 800\ \text{cm}^{-1}$ and the condition (4.3) leads to the requirement $\tau \ll 10^{-4}$ s (the fact that for water $\chi \ll \nu \approx 0.01\ \text{cm}^2/\text{s}$ has been taken into account). For visible and near infrared radiation, in cases of practical interest the dimension $l_{\min} \sim 1$ mm. In this case, the condition (4.3) for water is satisfied only for infrasound.[12)]

The relative contribution of the thermal and striction mechanisms is determined by the ratio between the second and third terms on the right side of Eq. (4.2). In order to establish this ratio, we shall examine the typical situation for observing optoacoustical effects in absorbing media, when the exciting optical beam (or several combined beams) is incident on the boundary of a liquid from a transparent medium (for example, air). The boundary of the liquid can be either free or covered with a transparent solid plate (the walls of a cuvette), while the region in which the radiation is absorbed—"the sound antenna"—in adjacent to the surface of the liquid. Depending on the ratio between the radius of the light beam r_0 and the mean free path of a photon in the liquid K^{-1}, the sound antennas can have different geometric shapes: for $Kr_0 \gg 1$, they are shaped like a "disc"; for $Kr_0 \ll 1$, they are shaped like a "needle"; for $Kr_0 \sim 1$, the sound antenna has the same sizes in all dimensions. [Here and everywhere below, it is assumed that the duration of the optical radiation $\tau \gg (cK)^{-1}$]. We note that in the case of transparent liquids, in which radiation can be focussed into the bulk of the liquid without significant energy losses in propagating to the focal region, the optoacoustical effects are usually observed by varying the focussing "depth" (observations of stimulated Mandel'shtam-Brillouin scattering, accompanying the generation of hypersound; excitation of sound and shock waves with optical breakdown in transparent liquids). In this case, the shape and dimensions of the sound antenna are determined by the shape and dimensions of the focal region.

Let us first examine the optical generation of sound pulses by a quasimonochromatic optical pulse with duration τ.[13)] In this case, we have

$$|\Delta\langle E^2\rangle| \sim \left(\frac{1}{r_0^2}+K^2\right)E_0^2 \sim \left|\frac{8\pi}{cn}\frac{1+(Kr_0)^2}{r_0^2}q_0\right|, \qquad \left|\frac{\partial Q}{\partial t}\right| \sim \frac{Kq_0}{\tau},$$

where $n \equiv \sqrt{\varepsilon}$ is the index of refraction of the medium and q_0 is the maximum intensity of the optical pulse. The ratio

$$\left|\frac{(\alpha/C_p)\,\partial Q/\partial t}{(8\pi)^{-1}(\rho\,\partial\varepsilon/\partial\rho)_T\,\Delta\langle E^2\rangle}\right| \sim \frac{\alpha r_0 nc}{C_p(\rho\,\partial\varepsilon/\partial\rho)_T\,\tau}\,\frac{Kr_0}{1+(Kr_0)^2}. \tag{4.4}$$

It is a maximum for $Kr_0 \sim 1$ (an equidimensional sound antenna). In this case, the thermal mechanism for generating sound is dominant, if

$$\tau \ll \frac{\alpha r_0 nc}{2C_p(\rho\,\partial\varepsilon/\partial\rho)_T}. \tag{4.5}$$

For example, for water with $r_0 \gtrsim 1$ MM we obtain the estimate $\tau \ll 15$ ms.

For "disc-shaped" and "needle-shaped" sound antennas, the estimate of the duration τ becomes more rigorous [the factor 1/2 is replaced by the factors $(Kr_0)^{-1}$ and (Kr_0), respectively, small in comparison with unity].

In this manner, it may be roughly assumed that for optical generation of sound pulses in absorbing liquids the thermal mechanism dominates for pulsed durations $\tau \sim 1$ ms and shorter.

Let us now discuss the optical excitation of quasimonochromatic sound waves with frequency Ω and wavelength $\lambda_\Omega = 2\pi/k$, where k is the wave number. For the striction mechanism, such sound waves can be excited as a result of the propagation of two light beams

[12)]We note that the condition (4.3), which represents the condition that thermal conductivity and viscosity have a small effect on the efficiency of the thermal mechanism for generating sound, provides a lower limit to the frequency of sound Ω. The same transport processes, as is well-known, provide an upper limit to the sound frequency by the condition that the absorption of the sound wave is small (i.e. by the condition $\Xi\Omega \ll 1$): $\Omega \ll \{u^2/\chi,\ u^2/\nu\}$. For most liquids, this condition is satisfied up to hypersound.

[13)]It is assumed that the time τ determines both the duration of the optical pulse, as well as the width of its front and trailing edges ("bell-shaped" pulse).

in the medium, intersecting at an angle θ with frequencies ω_1 and ω_2, such that $\omega_1 - \omega_2 = \Omega$; $2(\omega_{1,2}/c)n\sin(\theta/2) \approx k$. In this case, it is evident that

$$|\Delta\langle E^2\rangle| \sim (r_0^2 + k^2 + K^2)\, E_0^2 \sim \frac{8\pi}{nc} q_0 \frac{1 + (r_0 k)^2 + (r_0 K)^2}{r_0^2}.$$

For the thermal mechanism, it is also possible to use two intersecting light beams or a single beam with intensity modulated in time (with frequency Ω). The latter method will be discussed in detail below. The possibility of generating sound in the region of interference of two coherent light beams was discussed in Refs. 37–40. This phenomenon was studied experimentally in Refs. 39 and 41 (a train of pico-second pulses) and in Refs. 40, 42, 43 (a single pulse separated into two intersecting beams).

Without going into details, we note that in any of the cases cited above, involving the thermal mechanism for generating sound, the relationship $|\partial Q/\partial t| \sim K\Omega q_0$ is valid. Now, it is simple to generalize the estimate (4.4) to the case of monochromatic sound ($\tau \to \Omega^{-1}$; $1 + (Kr_0)^2 \to 1 + (kr_0)^2 + (Kr_0)^2$. It is evident that the striction mechanism becomes significant in the case of sufficiently low and sufficiently high sound frequencies Ω. For low frequencies, the boundary is established by the condition (4.5) with the substitution $\tau \to \Omega^{-1}$, inasmuch as in this region $r_0 k \equiv (r_0/u)\Omega \ll 1$. With an increase in the frequency Ω, the role of the thermal mechanism at first increases, and then in the region of frequencies for which $r_0 k \gg 1$ and $k \gg K$, it begins to decrease. It still dominates in this case under the condition that

$$\Omega \ll \frac{\alpha n c u^2 K}{C_p\,(\rho\,\partial e/\partial\rho)_T}.$$

For water with $K \gtrsim 0.2\ \mathrm{cm}^{-1}$ we obtain the estimate $\Omega \ll 10^9\ \mathrm{s}^{-1}$.

In this manner, it may be roughly assumed that, for optical excitation of quasimonochromatic sound waves in absorbing liquids, the thermal mechanism dominates for frequencies $f = \Omega/(2\pi)$ ranging from 10^2 to 10^9 Hz.

b) Propagation of sound. The near and far wave zones

Let us now estimate the magnitude of the pressure pulses that are generated in the liquid as a result of the absorption of laser radiation and their transformation as they propagate to distances that are large in comparison with the characteristic dimensions of the problem. We begin our analysis with the case of the generation of pressure pulses in the near-surface layer of a liquid (the near wave zone). For simplicity, we will assume that the following conditions are satisfied: $Kr_0 \gg 1$ and $r_0 \gg u\tau$, where τ is the duration of the laser pulse. This allows considering the problem as one-dimensional. Further, let L be the characteristic dimension of the region encompassed by the perturbation in the time τ:

$$L = \begin{cases} K^{-1} & \text{for} \quad u\tau K \ll 1, \\ u\tau & \text{for} \quad u\tau K \gg 1. \end{cases}$$

The characteristic magnitude (amplitude) of the pressure created in the liquid by the laser pulse is given by the product of the Grüneisen constant Γ_0 and the volume density of the input energy [see Eq. (2.15)], i.e.,

$$p' = \Gamma_0 A q_0 \tau \frac{1}{L}. \tag{4.6}$$

The simple estimate (4.6) coincides in accuracy with the amplitude of the pressure pulses obtained in Ref. 44 as a result of a rigorous solution of the equations of hydrodynamics. However, in deriving (4.6) and in contrast to Ref. 44, we did not make use of any particular mechanisms for generating sound. Thus, Eq. (4.6) remains valid both for the "thermal" as well as the "striction" mechanisms for exciting sound. In the latter case, the existence of a nondissipative "extinction" of the electromagnetic wave, arising from the "transfer" of electromagnetic energy into sound energy as a result of the striction effect, should be taken into account in determining K.

It is physically evident that when radiation acts on the free surface of a liquid the compression pulse must be replaced by a rarefaction pulse, which has approximately the same amplitude and duration. When the radiation acts on the surface of the liquid that is bounded by a rigid surface (the wall of a cuvette) the rarefaction pulse must be absent. Rigorous calculations[44] verify the correctness of these deductions.

Let us make some remarks concerning the duration of the pressure pulses τ_p. The problem being analyzed has two characteristic times: the duration of the laser pulse τ and τ_S, the time required for the sound wave to traverse a distance $\sim K^{-1}(\tau_S \sim (uK)^{-1})$. When $\tau \ll \tau_S$, the duration of the pressure pulses $\sim\tau$. When $\tau \gg \tau_S$, two cases should be distinguished: for a rigid boundary the pressure pulses excited in the liquid and reflected from the boundary have the same sign and duration $\sim\tau$; for this reason, the duration of the pulse arising as a result of their interference also will be $\sim\tau$. For a free surface, as a result of the interference of generated and reflected pulses, which have different signs, a pulse with mixed polarity and duration $\sim\tau_S$ arises. Let us estimate the efficiency for conversion of radiation energy into sound energy η:

$$\eta \equiv \frac{(u\rho)^{-1}\int_0^\infty [p'(t)]^2\,dt}{\int_0^\infty q(t)\,dt} \approx \frac{A^2\Gamma_0 q_0}{\rho u^3}\frac{\tau\tau_p u^2}{L^2}.$$

From here, we obtain for $u\tau K \ll 1$

$$\eta \approx A^2 \frac{\Gamma_0^2 q_0}{\rho u^3} u\tau K. \tag{4.7}$$

For $u\tau K \gg 1$, the conversion coefficients for the cases of a rigid and free surface are different due to the different values of τ_p.

For a rigid surface

$$\eta \approx A^2 \frac{\Gamma_0^2 q_0}{\rho u^3}.$$

For a free surface

$$\eta \approx A^2 \frac{\Gamma_0^2 q_0}{\rho u^3}\frac{1}{u\tau K}. \tag{4.8}$$

Comparing (4.7) and (4.8), we conclude that the conversion coefficient for a free surface must have a maximum for $u\tau K \sim 1$. In general, the expression for η has the form[44]

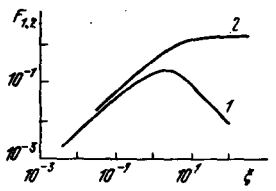

FIG. 8. The conversion efficiency factor F. 1—free surface, 2—rigid boundary; $\xi \equiv u\tau K$[44].

$$\eta = A^2 \frac{\Gamma_0^2 q_0}{\rho u^3} F(u\tau K), \tag{4.9}$$

where $F(u\tau K)$ is a universal dimensionless function. A graph of the function $F(u\tau K)$ is presented in Fig. 8.

It is evident from (4.9) that the conversion coefficient increases with an increase in the radiation intensity. However, it is not possible to increase the coefficient significantly in this manner, since the processes of vapor formation, which were not taken into account in this analysis, begin to play the dominant role at sufficiently large intensities.

As an example, we present the value of the conversion coefficient for water:

$$\eta_{H_2O} = 1.83 \cdot 10^{-11} q_0 F(u\tau K),$$

where q_0 has the dimension W/cm^2.

In analyzing the phenomena that occur in the far wave zone at distances from the center of the focal spot large in comparison with r_0 and K^{-1}, it is necessary to take into account the fact that the sound wave changes into a spherical wave, so that in its amplitude must decrease like r^{-1} in order to conserve the flux of sound energy. For this reason, in the far wave zone an additional factor r_0/r appears in the estimate (4.6). In addition, it is necessary to take the directivity of the sound antenna into account, which leads to the appearance of $f(\mathbf{n})$, a dimensionless function that depends on the direction of the observation point (directivity pattern). The function $f(\mathbf{n})$ satisfies the following normalization condition:

$$\int_{2\pi} f(\mathbf{n})\, do = 1,$$

or a similar condition, the precise form of which depends on the formulation of the problem. For a rectangular laser pulse, when the observation point lies along the axis of the laser beam $f(\mathbf{n}) \sim Kr_0$,[45] so that as a whole the amplitude of the pressure pulse $p' \sim \Gamma_0 K r_0 (A q_0 \tau / L) r_0 / r$, i.e., it is proportional to $A q_0 r_0^2$, the total laser power absorbed by the liquid. This value for p' is attained at time $t \sim r/u$. A strictly spatial problem concerning the optical generation of pressure pulses is solved in Ref. 46.

Let us now consider the process for generating monochromatic sound.[45] We shall assume that at the instant $t = 0$ a beam of optical radiation is incident normally on the planar surface of a liquid that occupies the half space $z > 0$. The intensity of the beam in the plane $z = 0$ has the form

$$q(\mathbf{r})(1 + m\cos\Omega t), \quad \mathbf{r} = \{x, y\},$$

m is the modulating factor $0 \leq m \leq 1$. The process leading to the steady state for the modulated beam are qualitatively the same as for the unmodulated beam and are described above. For this reason, we shall immediately go on to the analysis of the stationary regime for generating monochromatic sound. Inasmuch as, the basic mechanism for generating sound in the most interesting frequency range is the "thermal" mechanism as is shown above, we limit our analysis to this range. In addition, for simplicity, we assume that the beam has a Gaussian intensity distribution, i.e.,

$$q(\mathbf{r}) = q_0 e^{-(r/r_0)^2}.$$

In what follows, we examine the case of a free liquid surface and we assume that the distance R between the point of observation and the region in which heat is liberated is large in comparison with the dimensions of this region ($R \gg r_0$, K^{-1}).

In the far wave zone, where

$$R \gg k(r_0 \mathbf{n}_\parallel + K^{-1}\mathbf{n}_\perp)^2,$$

where $\mathbf{n}_\parallel$ and $\mathbf{n}_\perp$ are the components of the unit vector $\mathbf{n} \equiv \mathbf{R}/R$ along the Z axis and in the surface of separation ($Z = 0$), respectively, the solution to the equations of hydrodynamics has the form of a spherical wave

$$p_k'(\mathbf{R}, t) = -\mathrm{Re}\{p_k'(\mathbf{R}) \exp[i(k\mathbf{R} - \Omega t)]\}.$$

For the wave amplitude $p_k'(\mathbf{R})$ we obtain

$$p_k'(\mathbf{R}) = \frac{Am\alpha u}{2\pi C_p} \frac{Kk^2}{K^2 + k^2} \frac{e^{-\gamma R}}{R} P f(\mathbf{n}). \tag{4.10}$$

Here, $\gamma \equiv k\Omega\Xi$ is the amplitude absorption coefficient for sound and $P \equiv q_0 \pi r_0^2$ is the total power of the laser beam. The directivity pattern is determined by the expressions

$$f(\mathbf{n}) = f_1(\theta) F(\mathbf{k}_\perp), \quad f(\theta) = \frac{1 + (k/K)^2}{1 + (k/K)^2 \cos^2\theta} \cos\theta,$$
$$F(\mathbf{k}_\perp) \equiv \exp\left[-\left(\frac{kr_c \sin\theta}{2}\right)^2\right], \tag{4.11}$$
$$\mathbf{k}_\perp \equiv k\mathbf{n}_\perp, \quad |\mathbf{n}_\parallel| \equiv \cos\theta, \quad |\mathbf{n}_\perp| \equiv \sin\theta.$$

We will examine several limiting cases.

1) *Narrow beam ($kr_0 \ll 1$).* In this case, $F(\mathbf{k}_\perp) \approx 1$, while $f(\mathbf{n}) \approx f_1(\theta)$. For $k \ll K$, $f(\mathbf{n}) \approx \cos\theta$, i.e., the directivity pattern coincides with the directivity pattern of an acoustical dipole, which is understandable since all the dimensions of the region in which heat is liberated in this case are small in comparison with the sound wavelength, i.e., this region represents an acoustical point monopole. The analysis of a point monopole, situated on a free surface, is the same as the analysis of a dipole in a uniform medium.[47]

As the modulation frequency increases (i.e., with an increase in k), as is evident from (4.11), the function becomes more complicated, but the maximum in the directivity pattern coincides with $\theta = 0$ up to $k = K$. For $k \gg K$, the maximum in the directivity pattern occurs at an angle $\theta_M = \arccos(K/k)$. At $k \gg K$, the directivity pattern corresponds to the radiation emitted by a long (in comparison with the wavelength) chain of coherent monopoles, situated along the axis of the laser beam, and a chain of imaginary monopoles with opposite polarity, situated above the liquid surface, coupled with it. The emitted radiation has a narrow directional character: sound is emitted mainly along the surface of the liquid and uniformly in all directions. The direction of

the maximum forms an angle $\pi/2-\theta_M\approx K/k\ll 1$ with the surface of the liquid, and its angular width (at half-amplitude) is given by $\Delta\theta\approx 2\sqrt{3}K/k\ll 1$. The value of $f(\theta_M)\approx k/(2K)\gg 1$.

2) *Wide beam ($kr_0\gg 1$).* In this case the function $F(k_1)$ is significantly different from zero only for the angles $\theta\lesssim(kr_0)^{-1}\ll 1$, i.e., $f(\mathbf{n})\approx F(\mathbf{k}_\perp)$. The radiation is narrowly directed, but this time along the axis of the laser beam.

Using (4.12), we obtain in this case $f(n)=\exp[-(\theta/\Delta\theta)^2]$, where $\Delta\theta=2/(kr_0)$. The linear width of the "sound spot" at a depth R is given by

$$\Delta l=2R\Delta\theta=\frac{4R}{kr_0}.$$

We shall also clarify the problem concerning the optimal frequency of modulation $\Omega_{\rm opt}$, so that the amplitude of sound at a given point of observation R would be a maximum. We limit ourselves to the case that the observation point lies in the direction of the maximum in the directivity pattern and the maximum itself is situated at $\theta=0$. In this case, with the usual power law dependence for the dispersion coefficient ($\gamma(k)\sim k^\nu$; $\nu\approx 2$), the maximum for the expression (4.10) occurs for $k=k_{\rm opt}\equiv Kg(\Delta_0)$. Here, $\Delta_0\equiv\gamma(K)R$, while $g(\Delta_0)$ is a slowly varying function (according to a power law).

However, it is significant that in the most interesting case, when $\Delta_0\ll 1$, any noticeable increase in $p_k'(\mathbf{R})$ with an increase in k ceases for $k\sim K$. For further increase in k up to the value $k_{\rm opt}$, which satisfies the condition $\gamma(k_{\rm opt})R\sim 1$, the magnitude of the pressure increases slowly, after which an exponential decrease in $p_k'(\mathbf{R})$ begins [see (4.10)]. In other words, for $\Delta_0\ll 1$ the magnitude of the pressure over a wide range of frequencies $uK<\Omega<\Omega_{\rm opt}$ depends weakly on Ω and is close to $p_{k\,{\rm opt}}'(\mathbf{R})$. The case in which $\Delta_0\gtrsim 1$ has little interest, since sound in this case is strongly damped even at the optimum frequency.

The total energy flux P_S, removed by the sound, can be obtained from (4.10) by substituting $\gamma=0$ and integrating over the entire solid angle for the half space $Z>0$. Knowing P_S, it is easy to obtain the value of the conversion coefficient $\eta\equiv P_S/\pi r_0^2 q_0$. As an example, we present the value of η for a wide beam ($kr_0\gg 1$):

$$\eta=\frac{q_0 u}{\rho}\left(\frac{Am\alpha}{2C_p}\frac{Kk}{K^2+k^2}\right)^2. \tag{4.12}$$

From (4.12), it is evident that the maximum efficiency corresponds to the case $k=K$.

We shall now examine the near wave zone, where the observation point is located under the spot being irradiated ($r\lesssim r_0$) at a depth $L\ll kr_0^2$ [however, as before, $L\gg K^{-1}$ and $L\gg r_0$, so that it is possible to assume at the same time that the conditions for Fresnel diffraction are satisfied, $L\gg kr_0^2/(KL)$, $L\gg kr_0^2(r_0/L)^2$]. In this case, the sound wave has the form of a plane wave with an amplitude

$$p_k'(r)=\frac{Am\alpha u}{C_p}\frac{Kk}{K^2+k^2}q_0e^{-\gamma L}e^{-(r/r_0)^2}. \tag{4.13}$$

In the near zone, the beam does not have time to diverge and its width (according to the amplitude of the pressure) coincides with the width of the laser beam (according to intensity). We note that while in the far zone, where the sound wave is spherical, the amplitude $p_k'(\mathbf{R})$ is determined by the total power of the laser beam P [see (4.10)], in the near zone the amplitude of the sound is determined by the intensity $q_0=P/(\pi r_0^2)$.

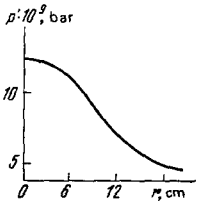

FIG. 9. The amplitude of the sound wave in the near wave zone.[48] Water; $L=75$ cm; $k=1.25$ cm^{-1}; $K=0.17$ cm^{-1}; $r_0=12$ cm; $q_\Omega=(15\pm 3)\cdot 10^{-3}$ W/cm^2.

An analysis of the frequency dependence of (4.13) shows that $k_{\rm opt}$ is significantly different from K only for the uninteresting case of large Δ_0.

The generation and propagation of monochromatic sound in a liquid (water) as a result of the absorption of laser radiation was studied experimentally in Ref. 48. In order to excite sound waves, a single mode YAG:Nd^{+3} laser at a wavelength of 1.06 μm was used. The intensity of the radiation was modulated with a Pockels cell, to which a sinusoidal voltage was applied so that the output radiation had the form

$$q(t)=q_0\left[1-\sin^2\left(\frac{\pi}{2}\sin\Omega t\right)\right], \tag{4.14}$$

where Ω is the modulation frequency. The amplitude of the sound was measured with a hydrophone, the signal from which was input to a two-dimensional automatic recorder after amplification and phase demodulation. The results of the measurements in the near and far wave zones exhibited good agreement between the experimental values and the values computed according to Eqs. (4.10) and (4.13).

Figure 9 shows the amplitude of the sound wave with frequency Ω [the first Fourier component of the nonmonochromatic signal with the modulation (4.14)] as a function of the distance from the center of the sound beam [$q_r\equiv 0.64q_0$ is the amplitude of the fundamental in the expansion of (4.14) in a Fourier series]. The amplitude of the sound wave on the beam axis, computed according to formula (4.13), in this case constitutes $(12.5\pm 2.5)\cdot 10^{-9}$ bar.

Figure 10 shows the theoretical dependence of the

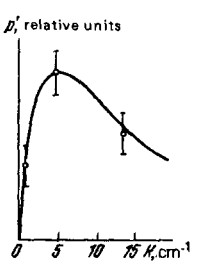

FIG. 10. The dependence of the sound amplitude in the far zone on the absorption coefficient for radiation. Water; $L=75$ cm; $k=4.2$ cm^{-1}; $r_0=2$ cm.[48]

sound amplitude in the far wave zone on the absorption coefficient for radiation in water and the corresponding experimental values ($L = 75$ cm, $k = 4.2$ cm^{-1}, $r_0 = 2$ cm, so that $L \gg kr_0^2$, i.e., the far zone, and $kr_0 \gg 1$, i.e., a wide beam; K was varied over the range 1 to 12 cm^{-1}). As follows from previous remarks, the sound amplitude has a maximum for $k \sim K$. The experimentally observed divergence in the sound beam for the same values of L, k, r_0, and K constituted 0.19–0.2 deg. The computed value of the divergence in these cases constituted 0.23 deg. In this manner, within the experimental accuracy, the results of the measurements coincide with the theoretical predictions, which indicates the correctness of the theoretical description of the phenomenon.

Under actual conditions, the effect of spatial fluctuations in the intensity of laser radiation, as well as the rippling of the free liquid surface, may be important in generating monochromatic sound. The role of these factors was analyzed in detail in Refs. 45, 46, 49, and 50. The influence of bubbles arising from gases dissolved in the liquid on the conditions of laser generation of sound and so on were studied in Ref. 51.

Of great interest are the results obtained recently by scanning laser radiation along the surface of a liquid. This is a unique method for obtaining an extended sound source, moving with practically an arbitrary Mach number, the motion of which is not related to any flow around the body of the emitter.[52-54] However, it is not possible for us to give a detailed discussion of this work.

5. DEEP MELTING PENETRATION OF METALS

In the final two chapters of this review we shall examine the problem of the interaction of radiation with metallic melts.

One of the interesting and important, for applications, problems in this area is the problem of the so-called deep or dagger-shaped melting penetration. The essence of this phenomenon consists in the following. An analysis of the dependence of the depth h of melting penetration into a metallic target by laser radiation as a function of the radiation intensity in the focal spot with a pulse having constant duration and as a function of the location of the focal point of the lens relative to the irradiated surface yields the following picture. At first, a slow increase in h is observed with an increase in the radiation intensity q. Metallographic analysis of the melting zone shows that the shape of the melting zone is at this stage similar to the situation in which the surface of the sample is heated by a heat source[14)] that has the dimensions of the focal spot and an intensity Aq.[32,55]

However, when some characteristic value of the intensity $q = \bar{q}$ is attained, the behavior of the function $h(q)$ changes sharply: the depth of the melting penetration begins to increase significantly more rapidly with an increase in q while the melting zone itself acquires a shape that is elongated in the direction of the laser radiation (this is the origin for the name of the phenomenon, viz. deep or dagger-shaped melting penetration). Typical functions $h(q_0)$ for a series of metals, as well as a metallographic picture of the melting penetration zone is shown in Fig. 11 and 12. Experiments were performed with metals having commercial-grade purity using the UL-20 laser setup[56] (pulse duration $\tau = 1.45$ ms) and the SLS-10-1 laser setup[57,58] with a smooth, nearly rectangular pulse shape with $\tau = 2$ and 4 ms.

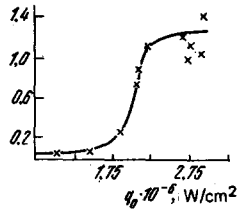

FIG. 11. The depth of melting penetration into copper as a function of the radiation intensity (stationary target).[56]

An analysis of the dependence of the depth of melting penetration on the position of the focal point of the lens, converging the laser beam relative to the surface of the sample, showed that the maximum depth is attained when the focal point is situated not on the surface of the sample, but rather beneath it.[56] The indicated dependence is shown in Fig. 13.

In order to understand all of these phenomena we note

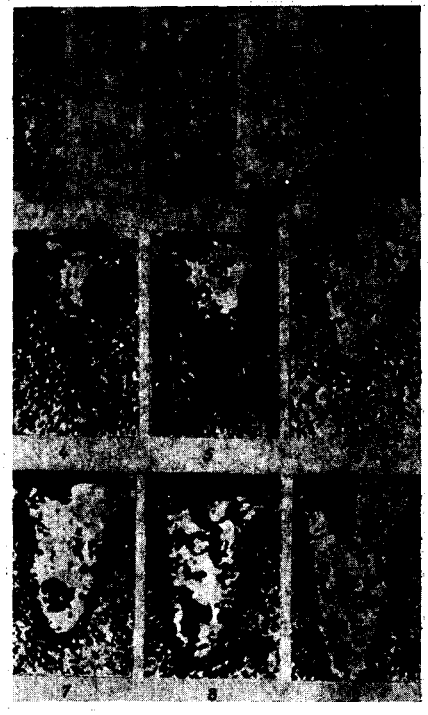

FIG. 12. The structure of the melting penetration zone in titanium for different values of the radiation intensity (stationary target[57]). q_0 (10^5 W/cm^2) = 0.59 (1), 1.1 (2), 2.3 (3), 2.7 (4), 3.1 (5), 4.1 (6), 5.2 (7), 6.0 (8), and 7.4 (9).

14)The path length for radiation in the case being examined is always small in comparison with characteristic dimensions of the problem, so that it can be assumed that the energy in the laser pulse is deposited directly on the surface of the target.

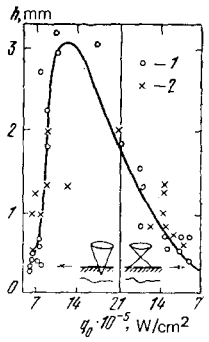

FIG. 13. The dependence of the melting penetration depth in aluminum as a function of the average intensity of illumination in the irradiated zone for different positions of the focal point of the lens relative to the surface of the target. Stationary target. Pulse energy 15 J. 1—lens with $F = 34$ mm, 2—same with $F = 50$ mm.[56]

that for the laser radiation intensities examined (10^6–10^7 W/cm^2) the melting of metals is always accompanied by the existence of three phases: solid, liquid, and vapor; and, in addition, since the intensity of the vapor formation increases extremely rapidly with an increase in the surface temperature, the vaporization process occurs mainly on a small part of the surface of the molten metal, located near the center of the focal spot and having, as a result, the highest temperature.

It is natural to assume that for $q = \tilde{q}$ the free surface of the melt is strongly indented, forming a funnel, as a result of the recoil force of the vapors from the sample. At the same time, the molten metal is pushed out of the melting zone, which lowers the effective heat source beneath the surface of the sample, and so on. Such a funnel-shaped indentation of the free surface of an absorbing liquid when laser radiation is focused on it was observed in Ref. 15 (Fig. 14). After the action of the laser pulse ceases, the melt that was first pushed out of the melting zone fills the crater once again and crystallizes there.

In this manner, the phenomenon of the deep melting penetration arises from the interaction of the laser radiation with the liquid phase (melt) of the metal. At the same time, all the qualitative features of the phenomenon can be explained within the framework of the indicated treatment: the presence of a threshold

FIG. 14. A laser funnel in glycerine. A continuous CO_2 laser. Stationary target $r_0 \approx 4 \cdot 10^{-2}$ cm; $q_0 \approx 10^5$ W/cm^2. Funnel depth approximately 20 cm.[59]

value for the laser radiation intensity $\tilde{q}$, as well as the dependence of the melting penetration depth on the position of the focal point of the lens relative to the surface of the sample (see below for greater detail).

Deep melting penetration is not the only phenomenon that results from the presence of a liquid phase in the irradiation zone. Thus, for example, the authors of Ref. 60 investigated the process causing the formation of a crater in a metallic target due to the removal of the liquid phase from the melting zone by the recoil pressure of the vapors, and they estimated the rate at which the depth of the zone increases at the stage of the process when this depth is small in comparison with the diameter of the focal spot so that the problem can be considered as being one-dimensional. The influence of the liquid phase on the formation of a crater with arbitrary depth is discussed in Ref. 61.

Here, however, we shall consider in detail only the problem of deep melting penetration, which, on the one hand, is very important for applications,[62,63] and on the other hand, is entirely relevant to the subject of this review, since all the main features of the phenomenon are explained by processes that occur at the liquid-vapor boundary, while the existence of the second phase boundary (solid-liquid) can be completely neglected.

We note that although the connection of the phenomenon with the presence of molten metal in the irradiation zone was indicated in Ref. 56, attempts to describe it quantitatively have only been made recently. Thus, a model was proposed in Ref. 57 and 64, in which the process of deep melting penetration was explained by a periodic displacement of the liquid phase from the bottom of the crater. It was proposed that the vaporization front is stationary until some characteristic temperature is attained at the surface of the liquid (the temperature of developed vaporization). After this, as a result of intensive vaporization, the "hot" layer of the melt is removed from the crater by the recoil pressure of the vapors and the process is repeated. In spite of the evident crudeness of this model, the authors of Ref. 57 and 64 were able to obtain satisfactory agreement with experiment for the dependences of the rate of melting penetration on the laser radiation intensity that they computed on the basis of this model.

We also note Ref. 124, in which a complete quantitative analysis of the physical phenomena related with the process of deep melting penetration (using laser as well as electron beam action) and in which simple estimates of the various parameters of this process were obtained. We also note Ref. 126, in which the plasma and gas dynamic phenomena in the crater arising with developed deep melting penetration were analyzed.

We emphasize that a rigorous approach to the problem of deep melting penetration in general involves the solution of a multidimensional self-consistent problem in optics, hydrodynamics of the flow of molten metal, kinetics of vaporization, and the hydrodynamics of vapor expansion. The difficulties that are encountered along the way, are so great that it is hardly possible

to progress beyond course estimates without extensive use of numerical methods.

However, it is significant that the practically important problem concerning the magnitude of the threshold for deep melting penetration can be solved in a rigorous manner without the use of questionable or poorly substantiated assumptions. In addition, since the solution to this problem simultaneously clarifies all the important features of the physics of the deep melting penetration phenomenon, we have considered it useful to examine this problem in greater detail, using the approach developed in Ref. 65.

Following this work, we now study the deformation of the free surface of the melt by the recoil vapor pressure in a stationary melting regime for the metallic sample, which is motionless relative to the laser target under the condition that $\chi\tau \gg r_0^2$.

We shall use perturbation theory, neglecting the differences in the thermophysical properties of the solid and liquid phases. Since we are particularly interested in the melting of the sample, it is natural to examine only such laser radiation flux densities that are less than the threshold for developed vaporization q_V.[32,66] At the same time, it is possible to neglect the motion of the melt, due to the removal of mass as a result of vaporization, as well as the energy expended on vaporization.[15)]

Approximating the free surface of the melt by the surface $z=0$, in the zeroth order approximation, we find that in this case the temperature distribution satisfies the Laplace equation for the half space $z>0$. For definiteness, let us assume that the laser beam has a Gaussian intensity distribution

$$q(r)=q_0 e^{-(r/r_0)^2}.$$

Then the temperature distribution along the surface of the target has the form

$$T(r)=T_s \exp\left[-\frac{1}{2}\left(\frac{r}{r_0}\right)^2\right] I_0\left[\frac{1}{2}\left(\frac{r}{r_0}\right)^2\right]+T_0, \tag{5.1}$$

where $T_S \equiv Aq_0 r_0\sqrt{\pi}/(2\varkappa)$, $I_0(x)$ is a modified Bessel function (for simplicity, we will assume everywhere below that $T_0=0$), while as a whole the temperature profile has the following asymptotic form:

$$T(r,z) \underset{R\to\infty}{\approx} \frac{T_s}{\sqrt{\pi}}\frac{r_0}{R}, \quad R\equiv\sqrt{r^2+z^2}, \tag{5.2}$$

which is satisfied with an accuracy not less than 5% for $R \geqslant 3$.

If the saturated vapor pressure of the sample $p_S(T)$ at the characteristic temperature $T=T_S$ is large in comparison with the external pressure, which is the case, as a rule, under real experimental conditions, then the recoil vapor pressure, with an error not exceeding several percent, is determined by a function valid for vaporization into a vacuum:

$$p=\frac{1}{2}p_s(T). \tag{5.3}$$

15)All the quantitative limitations that follow from the formulation of the problem will be presented below.

The true value of p deviates from Eq. (5.3) as a result of the presence of a flow of vapor atoms, returning to the surface as a result of collisions in the gas phase. But, in this case, this flow is always small,[32,67] which is what makes Eq. (5.3) applicable.

In Ref. 65, the Einstein model of a condensed body, in which the Einstein frequency was an adjustable parameter, was used to determine the function $p_S(T)$. However, it is better to use the function

$$p_s(T)=p_0 \exp\left(-\frac{\lambda_1}{T}+\frac{\lambda_1}{T_B}\right)\equiv p_0^* \exp\left(-\frac{\lambda_1}{T}\right), \tag{5.4}$$

which is obtained as a result of an approximate integration of the Clausius-Clapeyron equation with two adjustable parameters $p_0{}^*$ and λ_1 (see, for example, Ref. 66). In this case, $\lambda_1 \equiv \lambda A_m/N_A$ has the meaning of an atomic heat of vaporization, while p_0 and T_B denote the normal pressure and the normal boiling point.

We note that, in the case we are considering, the condition $\lambda_1 \ll T$ is always satisfied, so that the exponent entering into (5.4) is a rapidly varying function of temperature.

In the equilibrium case, the shape of the free surface of the melt is determined from the equality of the recoil vapor pressure of the sample and the hydrostatic pressure beneath the indented surface. We obtain the explicit function $p(r)$ by substituting the temperature $T=T(r)$, determined by Eq. (5.1) into Eqs. (5.3) and (5.4). From here, we immediately conclude that the characteristic range over which $p(r)$ decays equals

$$r_p \equiv r_0\sqrt{\frac{2T_s}{\lambda_1}} < r_0. \tag{5.5}$$

Knowing the function $p(r)$, it is possible to determine the shape of the free surface of the melt in the next approximation. Denoting the deviation of the points on the free surface from the plane $z=0$ for small curvatures of the surface (perturbation theory is applicable only in this case) as ζ, we have the following equation for the function ζ[68]

$$\begin{gathered}\Delta\zeta-a^2\zeta+\frac{1}{\sigma}p(r)=0,\\ \zeta(\infty)=0,\end{gathered} \tag{5.6}$$

where σ is the surface tension; a is the capillary constant ($a\equiv\sqrt{\rho g/\sigma}$, g is the acceleration of gravity, directed along the z-axis).

Equation (5.6) can be solved in general form,[16)] but for the subsequent analysis it is sufficient to limit ourselves to its asymptotic solution for $ar \ll 1$, since for metallic melts and actual sizes of the focal spot, the inequality $ar_0 \ll 1$ is always satisfied and the indicated asymptotic expression is valid up to the isotherms $T=T_m$, where T_m is the melting temperature.

16)The problem concerning the shape of the surface of the liquid phase is examined in Ref. 69, where the solution to Equation (5.6) is obtained for arbitrary $p(r)$, as well as for different examples of this function. However, in this reference, the relationship between the form of the function $p(r)$ and the parameters of the laser beam and the thermophysical properties of the melt is not established.

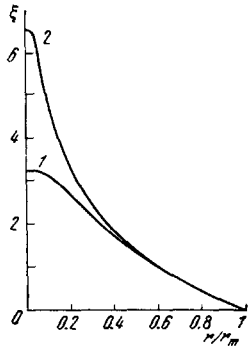

FIG. 15. The shape of the melt surface, deformed by the recoil vapor pressure. 2 corresponds to the greatest intensity ($1-\beta=3.8$; $2-\beta=19.6$); $\xi\equiv[\zeta(r)-\zeta(r_m)]/\zeta_0$.

This asymptotic expression has the form

$$\zeta(x)=\zeta_0\left[\mathrm{Ei}(-x^2)-2C-2\ln\frac{ar_p}{2}x\right],$$
$$\zeta_0\equiv\frac{T_S r_p^2 p_0^*}{4\sigma\lambda_1}e^{-\lambda_1/T_S},\qquad x\equiv\frac{r}{r_p}.$$

Here, $\mathrm{Ei}(-x^2)$ is the integral exponential function and C is Euler's constant ($C=0.57721\ldots$).

Figure 15 shows a graph of the function $\zeta(r)-\zeta(r_m)$, where r_m is the radius of the melt boundary ($T(r_m)=T_m$) for different values of the parameter β,

$$\beta\equiv\frac{r_m}{r_p}\approx\sqrt{\frac{Aq_0r_0\lambda_1}{4\sqrt{\pi}\,\varkappa T_m^2}}.$$

It is evident that even within the limits of applicability of perturbation theory the deformation of the free surface of the melt sharply increases near the axis of the laser beam with an increase in the radiation intensity.

By now requiring that the curvature of the free surface of the melt be small in comparison to r_p, which guarantees the applicability of perturbation theory, we obtain the condition $q_0<\tilde{q}$, where

$$\tilde{q}\approx\frac{6\lambda\rho\chi}{Ar_0\sqrt{\pi}}\left(\ln\delta_R-\frac{1}{2}\ln\ln\delta_R\ldots\right)^{-1},$$
$$\delta_R\equiv\frac{r_0p_0^*}{4\sqrt{2}\,\sigma}.$$

(we used the fact that for metals in a condensed phase the atomic heat capacity equals 3, so that $\varkappa=3\chi\rho N_A/A_m$).

It will be shown below that Eq. (5.7) simply determines the threshold for deep melting penetration. However, before going on to the rest of the analysis, we note that all the characteristic parameters of the problem, including also the quantity $\tilde{q}$, can be estimated on the basis of the following simple arguments: the radius of the focal spot r_0 is the characteristic dimension over which the temperature of the target changes in the given formulation of the problem. The characteristic temperature of the surface of the target can be found from dimensional considerations. Forming a combination from the quantities Aq_0, r_0, and $\varkappa$ that has the dimensions of temperature, we find that $T_S\sim Aq_0r_0/\varkappa$. In addition, since the temperature distribution along the surface of the target has a maximum at the center of the focal spot, by expanding $T(r)$ in a series with respect to powers of r, we find that near the maximum

$$T(r)\approx T_S\left[1-\frac{1}{2}\left(\frac{r}{r_0}\right)^2+\ldots\right]. \tag{5.8}$$

Substituting the series (5.8) into Eq. (5.4), which determines the temperature dependence of the saturated vapor pressure, we find that the characteristic dimension over which the recoil vapor pressure changes is $r_p=r_0\sqrt{2T_S/\lambda_1}$, which is identical in precision with expression (5.5). Since the deformation of the melt is due to the recoil vapor pressure, r_p is at the same time the characteristic dimension of the base of the funnel that arises at the surface of the melt. The depth of this funnel ζ_0 can be estimated from Eq. (5.6). Taking into account the fact that $\Delta\zeta\sim\zeta_0/r_p^2$ and that $r_p^{-2}\gg a^2$, we find from (5.6) that

$$\zeta_0\sim\frac{r_p}{\sigma}p(T_S)\sim\frac{T_S r_p^2 p_0^*}{\sigma\lambda_1}e^{-\lambda_1/T_S}. \tag{5.9}$$

The estimate (5.9) practically coincides with the quantity ζ_0, obtained above as a result of a rigorous solution of the problem.

Finally, the quantity $\tilde{q}$ is determined from the condition $\zeta_0\sim r_p$, which (to within a numerical factor of the order of unity) leads to the expression (5.7). We emphasize that Eq. (5.7) determines the laser radiation intensity that corresponds in the experiments to the threshold for deep melting penetration. In actuality, exceeding the intensity $\tilde{q}$ leads to a strong indentation in the free surface of the melt, which explains the appearance of the deep melting penetration (see the beginning of this chapter). With this, due to the sharp (exponential) dependence of ζ_0 on q_0, the condition $q_0<\tilde{q}$ actually has a threshold character, i.e., insignificant deviations of q_0 from $\tilde{q}$ lead to stricter inequalities for the compared quantities (r_p and ζ_0).

Let us now find the threshold for developed vaporization q_V. The integral energy flux, removed by heat transfer p_T, can be determined on the basis of Eq. (5.2). Taking into account the fact that the solid angle in which the heat transfer occurs equals 2π, we find that

$$P_T=2\sqrt{\pi}\varkappa r_0T_S\approx6\sqrt{\pi}\frac{\rho N_A}{A_m}\chi r_0T_S.$$

Neglecting the kinetic energy of the vapor particles in comparison with λ_1 and the return flow of atoms, in correspondence with earlier remarks, and taking into account the fact that the effective vaporization occurs from a spot with radius r_p, we find the following estimate for the integral flux of energy expended on vaporization $P_V=\pi r_p^2\lambda_1 j_V$ (j_V is the flux density of vaporized particles)

$$P_V=\pi r_p^2\lambda_1\frac{p_S(T_S)}{\sqrt{2\pi mT_S}}=\sqrt{\frac{2\pi N_AT_S}{A_m}}\,r_p^2p_0^*e^{-\lambda_1/T_S},$$

where $m\equiv A_m/N_A$ is the mass of an atom.

The threshold for developed vaporization q_V can be determined from the formal equality $P_V=P_T$. We have

$$q_V\approx\frac{6\lambda\rho\chi}{Ar_0\sqrt{\pi}}\left(\ln\delta_V+\frac{1}{2}\ln\ln\delta_V\ldots\right)^{-1},$$
$$\delta_V\equiv\frac{r_0p_0^*}{3\rho\chi\sqrt{2\lambda}}. \tag{5.10}$$

We note that the sharp dependence of P_V on T_S for comparatively slow dependence of P_T, just as in the

case of $\bar{q}$, ensures satisfaction of the stricter inequalities for the compared quantities with small deviation of q_0 from q_V.

The expression for q_V, obtained in Ref. 66 from dimensional considerations, differs from (5.10) by the absence of the numerical factor $6/\sqrt{\pi}$ and the expression in parenthesis.

It is evident from the remarks made above that the optimum values of q_0 for deep melting penetration occur in the interval $\bar{q} < q_0 < q_V$. Such an interval exists only if $\bar{q} < q_V$, which leads to the condition

$$\frac{\rho\chi\sqrt{\lambda}}{\sigma} > \frac{3}{4}[(\ln\delta_V + \ldots)(\ln\delta_R - \ldots)]. \tag{5.11}$$

We emphasize the weak dependence of the criterion (5.11) on the dimensions of the focal spot r_0. Physically, this indicates that the possibility for obtaining the optimal conditions for deep melting penetration are mainly determined by the thermo-physical properties of the sample and not by the properties of the laser beam.

Reference 65 compares the quantity $\bar{q}$, computed according to the method described above, for 13 metals with the results of experimental measurements of this quantity carried out in Refs. 56–58, and good agreement between theory and experiment is demonstrated. Typical values of $\bar{q}$ for $r_0 \sim 10^{-2}$ cm are of the order of 10^5 W/cm^2 for low-melting metals and 10^6 W/cm^2 for high-melting metals. The value of q_V, computed in Ref. 65 for the conditions of the experiments in Ref. 56–58, always exceed $\bar{q}$ by a factor 1.5–2.

Free oscillations of the surface of the melt were also studied in Ref. 65. Such oscillations lead to scattering of laser radiation. The crystallization of the melt, caused by such oscillations, can be explained by the presence of so-called "ring-shaped waves" on the surface of the melt, repeatedly observed experimentally (see the monograph in Ref. 61 and the references cited therein concerning this problem) and so on. It is shown that the maximum amplitude always occurs for the harmonic that corresponds with the smallest natural frequency of such oscillations and that for sufficiently large values of q_0 this amplitude increases mainly as the scale factor ζ_0, i.e., as $\exp[-6\lambda\rho\chi/(Ar_0\sqrt{\pi}q_0)]$.

The calculations presented above did not take into account the influence of hydrodynamic flow of the melt, caused by the removal of mass due to vaporization, on the formation of the temperature profile in the melt. This is permissible only to the extent that the effective coefficient of thermal diffusivity, due to this flow, is small in comparison with χ, i.e., if the inequality $Vr_0 \ll \chi$, where V is the speed of the vaporization front, is satisfied. Taking into account the fact that V is determined from the condition $V\rho = mj_V$, we obtain, in the approximation being considered,

$$V(T) = \frac{p_S(T)}{\rho}\sqrt{\frac{A_m}{2\pi N_A T}},$$

i.e., that the condition $Vr_0 \ll \chi$ is equivalent to the condition $P_V \ll P_T$ and does not contribute additional limitations to the problem at hand. In the case of developed vaporization, such a flow must be taken into account. The problem concerning the shape of the surface of the liquid phase in the limiting case of strong evaporation, when the hydrodynamics of the flow of the melt predominates, was discussed in Ref. 70. However, we note that if only the action of the radiation on the preliminarily melted metal (liquid mercury and so on) is of concern, then the temperature gradients will be very large with such large intensities, the melt layer will be thin, and, in essence, the problem reduces to the classical problem concerning the formation of a crater in a solid, for which the process of vaporization can be examined as sublimation, neglecting the existence of the liquid phase.[32,61]

6. METAL-DIELECTRIC TRANSITION UNDER THE ACTION OF LASER RADIATION

The idea of a transition of a liquid metal into a liquid nonmetallic phase was first proposed by Zel'dovich and Landau in 1943.[71] The idea was based on the fact that at high pressures and temperatures ~10^4 K the thermal excitation (and therefore, the conductivity as well) of dielectrics becomes so large that the difference between a dielectric and a metal, in essence, disappears. This makes it possible to bring about a continuous transition from the dielectric to the metallic phase and vice versa. But, then, at lower temperatures and pressures there can exist a line for the metal-dielectric transition terminating in a corresponding critical point, which, generally speaking, does not have to coincide with the line for the liquid-vapor phase transition.

An experimental study of the electrical conductivity of liquid metals[17)] has shown that near the critical point for the liquid-vapor transition a small change in the density of the metal leads to a sharp change in its electrical conductivity, and in addition, this occurs both for the supercritical state as well as for the subcritical state, i.e., in the liquid phase. According to the data in Ref. 72, a decrease in the density of mercury by 20% in the supercritical state leads to a drop in its electrical conductivity by four orders of magnitude. Approximately the same drop in electrical conductivity occurs also in the liquid phase of mercury when its density is decreased to half its normal value. It is evident from Fig. 16, that the temperature dependence of the relative electrical resistance of a sample with constant density near the critical point for the liquid-vapor transition has a form that is typical for dielectrics (sharp decrease in electrical resistance with an increase in temperature). This kind of behavior for the electrical conductivity suggests the existence of a critical point for a metal-dielectric transition. However, it should be emphasized that a change in the state of a metal occurs in a continuous, although sharp, manner. For this reason, in this case there is no phase transition line, which is replaced by some region of values for thermodynamic variables that has a small but finite width, i.e., the transition is diffuse.

With an increase in laser energy there appeared the

[17)]The most reliable data exist for mercury and cesium (see the review in Ref. 72 and the reference cited therein).

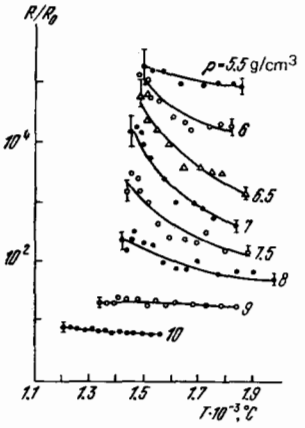

FIG. 16. Isochrones of the relative electrical resistance of mercury as a function of temperature. Mercury, $T_C - 1753 \mp 10$ K; $P_C = 1520 \mp 10$ bar; $\rho_C = 5.7 \mp 0.2$ g/cm^3.[73]

possibility of irradiating a metallic target in order to obtain temperatures and pressures corresponding to the critical values in the irradiation zone. For this reason, it was natural to make an attempt to study the influence of the metal-dielectric transition on the evolution of the interaction process between the laser radiation and the target material. This problem was first examined in Ref. 66 on the basis of a qualitative analysis of the phenomena that result from the appearance of a dielectric phase in the subcritical state of the metal. However, due to the complexity of the problem, the authors of Ref. 66 introduced a series of simplifying assumptions (in particular, concerning the transparency of the vapor), as a result of which the picture they presented concerning the interaction of the laser radiation with the target in the region of parameter values of interest to us was extremely simplified and far from reality in many of its details.

A rigorous analysis of the phenomenon, as noted in Ref. 74, is possible only on the basis of a numerical solution to the appropriate problem, taking into account a definite equation of state and a definite dependence of the abospriton coefficient and conductivity of the metal on temperature and density. This was done most systematically for the supercritical state of metals in Refs. 75–77, the results of which we will now discuss.

The following problem is examined theoretically in the references cited above. A uniform flux of radiation is incident from the vacuum onto the surface of a metal that occupies the half space $z < 0$. The radiation is partly absorbed and partly reflected. The intensity of the radiation is high enough to cause the temperature in the absorption region to attain (within the duration of the laser pulse) the critical temperature for the substance. The heated metal expands into the vacuum, forming a plasma flame, while the absorption zone shifts from the surface of the metal to the dense plasma region. A shock wave forms in the metal as a result of the action of the recoil pulse, arising with the expansion. The regime studied in Refs. 75 and 76 is similar to the one which is referred to as "slow combustion" in the hydrodynamics of burning.[68] In this case, the shock wave is weak, while the speed of motion of the absorption zone for the laser radiation ("combustion front") is subsonic.[18)] The qualitative picture of the process being considered is as follows. A weak shock wave propagates in the perturbed metal. Behind the shock wave, there is a compression region, which passes into a region where stress is intensively relieved. In the latter region, there occurs a transition of the dense metallic vapor into a rarefied vapor, which constitutes a plasma that is almost transparent to the laser radiation and that expands towards the laser beam. The boundaries between the regions are, to a significant extent, arbitrary. The separated surfaces are only the shock wave and plane, from which light is reflected, i.e., on which the real part of the dielectric permeability $\mathrm{Re}\,\varepsilon(\omega)$ vanishes.

The dimensions of all the indicated regions change with time and the problem as a whole is nonstationary. However, after the shock wave is separated from the stress-relieving wave and enters into the bulk of the substance, in a system of coordinates fixed to the reflecting surface, a stationary[19)] structure is established for the most interesting region of absorption of laser radiation, where the gradients of all the variables are large. Adjacent to the left of this region is the region of the substance compressed by the shock wave, in which the values of the hydrodynamic variables and also quasistationary; to the right, there is a region with a nonstationary flow, which is a self-similar, centered rarefaction wave.[20)] The profiles of the hydrodynamic variables in this wave and the coefficient of absorption of radiation can be written down in explicit form (the substance in the rarefaction wave constitutes an ideal equilibrium plasma). This permits the use of the values of the variables at the head of the rarefaction wave as boundary conditions for numerical integration of the equations that describe the stationary part of the flame.

In order to determine the equation of state, the coefficient of absorption, the thermal conductivity, and the other properties of the substance in the entire region of densities and temperatures required for calculations, the authors of Refs. 75–77 analyzed a large quantity of experimental data[73,79-82] and used the results of some theoretical calculations.[83-84] This permitted the use of a tabulated equation of state for the numerical integration of the equations together with analytic extrapolation and interpolation into regions for which

---

18)Such a "slow combustion" regime occurring in the case of interaction of laser radiation with matter was first studied in Ref. 78.

19)More precisely, the structure is quasistationary, since such a dependence will enter into the boundary conditions (see below), even though the equation that describes the change in the variables in this region does not depend on time, so that as a whole the solution will depend on time as a parameter.

20)Strictly speaking, the flow is not terminated with a rarefaction wave. For $z \to \infty$, this wave has a nonhydrodynamic "tail", which represents a free molecular flow.[67] However, the presence of such a "tail" has no effect on the problem being examined, since the mass contained in it and the fraction of radiation absorbed by it are neglible.

there were no experimental data.

As previously noted, the most complete experimental data concerning the equation of state and conductivity have been obtained for mercury. For this reason, the calculations were performed for this particular case. In order to obtain approximate equations of state for other metals, it is possible to use the principle of corresponding states. As shown in Ref. 85, such an approach is known to be applicable to metals for one group of the periodic system of elements and give good results for metals as a whole. In this manner, the data[75,76] acquire great generality, if the following dimensionless variables are introduced:

$$\tilde{\rho}=\frac{\rho}{\rho_C},\quad \tilde{T}=\frac{T}{T_C},\quad \tilde{p}=\frac{p}{p_K},\quad \tilde{q}=\frac{q}{q_K},\quad \zeta=\frac{z}{z_K},$$
$$p_K\equiv B\rho_C T_C,\quad q_K\equiv\rho_C(BT_C)^{3/2},\quad z_K\equiv\frac{T_C\varkappa_C}{q_K}\approx\frac{1}{3}\left(\frac{\pi}{e}\right)^2\frac{\sigma_C\sqrt{T_C}}{\rho_C B^{3/2}},\qquad (6.1)$$

where $B\equiv R/A_m$ is the reduced gas constant, σ is the conductivity, and e is the electronic charge. In the last equality appearing in (6.1), we made use of the Wiedemann-Franz ratio and expressed $\varkappa$ in terms of σ. The characteristic value for the radiation intensity q_K for a mercury target equals approximately 10^7 W/cm^2.

The typical structure of the absorption zone is shown in Fig. 17. For convenience, two scales are shown for q: the left scale uses dimensionless units (6.1), while the right scale corresponds to units of W/cm^2, for mercury; z is given in cm (for mercury). The rarefaction wave is adjacent to the right of the vertical line that bounds the region of the numerical computation. The reflection coefficient in this case equals 1%, while the optical thickness of the plasma flame $\Lambda=2.3$. The narrow zone near the surface $\mathrm{Re}\,\varepsilon=0$, in which the substance rapidly expands and is rapidly heated, is shown in greater detail in Fig. 18, in which, besides $\tilde{q}=18$ data are presented for $\tilde{q}=8.3$ and $\tilde{q}=31.6$. The weak dependence of the profile $\rho(z)$ for $z<0$ on the radiation intensity is explained by the small compressibility of the substance for $\rho>\rho_C$. On the other hand, the rate of expansion of the subst nce for $z>0$ increases sharply with an increase in $\tilde{q}$. The temperature profiles are also very sensitive to a change in the intensity (the temperature distribution in the region $z<0$, where radiation does not penetrate, is determined by

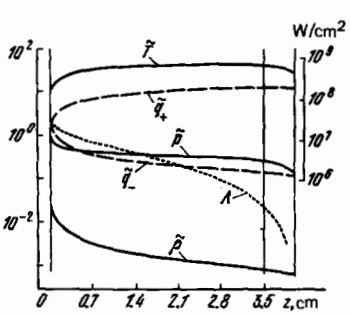

FIG. 17. The structure of the absorption zone for a rectangular laser pulse acting on a mercury target. $\tau=300$ ns; $\omega=1.78\cdot10^{15}$ s^{-1}; $q=18q\approx2\cdot10^8$ W/cm^2. $\tilde{q}_+$ and $\tilde{q}_-$ denote the incident and reflected fluxes, respectively. The origin of coordinates coincides with the surface $\mathrm{Re}\,\varepsilon=0$.[75]

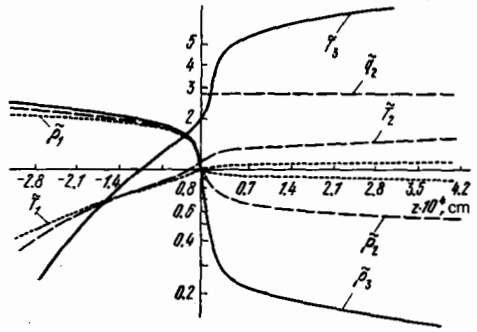

FIG. 18. The same as Fig. 17. The region near the reflecting surface is shown on a smaller scale. 1—$\tilde{q}=8.3$; 2—$\tilde{q}=18$; 3—$\tilde{q}=31.6$.[75,76]

the electronic thermal conductivity). The same flame structure is retained for a ruby laser as well. In the case of CO_2 laser radiation, the radiation is reflected from the hot rarefied plasma.

Let us now discuss the behavior of $\mathrm{Re}\,\varepsilon(z)$ and the metal-dielectric transition. For the case illustrated in Fig. 17, the value of $\mathrm{Re}\,\varepsilon$ at the head of the rarefaction wave, equal to 0.992, slowly decreases with an increase in the plasma density, and at a distance $\sim10^{-3}$ cm from the reflecting surface, $\mathrm{Re}\,\varepsilon=0.972$ (here $\tilde{T}=3.2$, $\tilde{p}=0.178$); then, in a narrow zone $\sim10^{-3}$ cm the substance becomes almost completely dielectric[21)] ($\mathrm{Re}\,\varepsilon=0.9993$, $\tilde{T}=1.4$, $\tilde{p}=0.51$), and immediately after this, the dielectric is transformed into a metal in a region with dimensions $\sim3\cdot10^{-5}$ cm and reflects the light completely ($\mathrm{Re}\,\varepsilon=0$; $\tilde{T}=1.16$; $\tilde{p}=1.6$). The coefficient of absorption of light K has a similar behavior. The function $K(\rho)$ in this case is illustrated in Fig. 19. If necessary, using Fig. 18, we can recompute it in terms of $K(z)$ or $K(T)$. Such a behavior for ε and K is explained by the simultaneous change in the temperature, density, and electronic concentration. But, it may also be explained qualitatively as follows (see Fig. 19): 1) the region ab corresponds to the appearance of a gap in the electronic spectrum (metal-dielectric transition); 2) bc corresponds to a gap that is completely open, but the temperature increases, and the conductivity increases with it;[79,84] the degree of ionization is small; 3) cd corresponds to the formation of plasma, the concentration of free electrons increases and K increases in spite of expansion; 4) de is a region with multiple ionization. The degree of ionization α_i increases slowly, and for this reason, K decreases as a result of expansion ($K\sim\rho^2\alpha_i^3T^{-3/2}$). The nonstationary part of the flame, corresponding to the rarefaction wave, is not shown in Fig. 19.

We emphasize that the density gradient is very large in the metal-dielectric transition region, while the temperature does not change as much, which is explained by the comparatively large thermal conductivity. For this reason, the formation of a sharp density front

[21)]The criterion for the substance to be considered as a dielectric is the vanishing of the plasma frequency, i.e., the absence of free electrons.

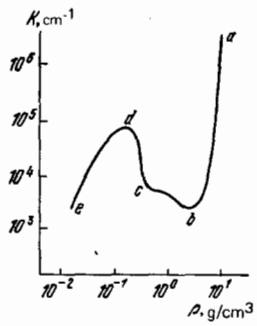

FIG. 19. The same as Fig. 17. The dependence of the coefficient of absorption of radiation on the density of mercury in the flame.[75]

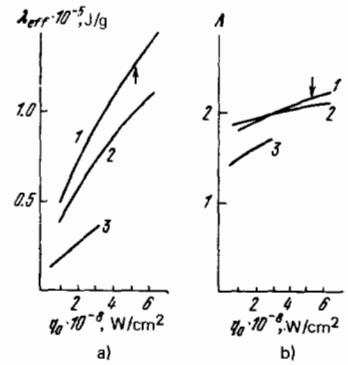

FIG. 20. The dependence of the effective heat of vaporization for mercury λ_{eff} (a) and the optical thickness of the flame Λ (b) on the radiation intensity. 1—$\tau = 300$ ns, $\omega = 1.78 \cdot 10^{15}$ s^{-1}; 2—$\tau = 300$ ns, $\omega = 2.713 \cdot 10^{15}$ s^{-1}; 3—$\tau = 10$ ns, $\omega = 1.78 \cdot 10^{15}$ s^{-1}. The arrow indicates the instant that the dielectric phase disappears.[75]

gives rise to a sharp change in the optical properties of the substance. Since the density gradient also increases with an increase in the radiation intensity (see Fig. 18), the width of the zone in which the substance is transformed into a dielectric in this case decreases. For intensities $\tilde{q} \geq 52$, the dielectric zone completely disappears, and the transparency of the plasma slowly decreases as the reflecting surface is approached, after which the plasma is sharply metallized, i.e., the function $K(z)$ becomes monotonic. We emphasize that at such intensities the plasma is heated to very high temperatures ($\tilde{q} = 52$ corresponds to $\tilde{T}(0) = 2.11$), and it is precisely this that explains the disappearance of the dielectric region: the hot dense plasma, which itself is not transparent, is compressed up to metallic densities.

When the radiation intensity is decreased, the width of the dielectric region increases. However, this phenomenon is weakly manifested, since there is a rarefied comparatively weakly ionized plasma in front of the dielectric phase, which is also almost transparent to the radiation.[22)]

Calculations of the effective specific energy of vaporization $\lambda_{eff} = q/j_m$, where $j_m \equiv mj_V$ is the mass flux density,[75] and of the specific recoil pulse[75,76] as a function of the intensity of the laser radiation (see Fig. 20 and 21) were performed. It is evident that both functions are monotonic and the presence of the dielectric phase has no effect on their behavior. The monotonic increase in λ_{eff} and the decrease of the specific recoil pulse with an increase in the laser intensity and pulse duration is explained by the fact that an increase in these parameters in the laser action regime of interest here leads to a "useless" increase in the dimensions of the flame and to an increase in its temperature, while the fraction of the energy expended on vaporization decreases. The decrease in λ_{eff} with an increase in the radiation frequency is related to the fact that the high-frequency radiation (ruby laser) is not absorbed as well ($K \sim \omega^{-2}$) and is reflected from the denser substance, while, since the optical thickness of the flame depends weakly on the characteristics of the laser pulse (see Fig. 20), a large fraction of the energy in the ruby laser radiation is deposited in the region that is optically inaccessible to the neodymium laser radiation. For this reason, ruby laser radiation destroys the target more effectively. We are not familiar with any experimental data concerning the quantity λ_{eff} in the range of radiation inte sities being considered. A comparison of the specific recoil pulse, computed in Refs. 75 and 76, with experiments performed with a series of metals,[32] shown in Fig. 21, demonstrates the good agreement (in order not to complicate Fig. 21 needlessly, we presented data only for An and Al). We note that the dependence of the specific recoil pulse on the radiation intensity, expressed in the appropriate dimensionless variables, is a universal function. This permits an immediate determination of two critical parameters, T_C and ρ_C, by comparing the experimental curve with that illustrated in Fig. 21 with the help of a scale transformation. After this, p_C is determined from the principle of corresponding states. This method can be used for determining the critical parameters of high-melting metals, which is difficult to do using other methods.

The stability of the stationary regime for the expansion of the flame examined in Refs. 75 and 76 was studied in a recently published work,[77] in which the nonstationary equations of hydrodynamics were numerically

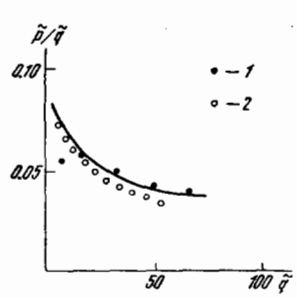

FIG. 21. The dependence of the specific recoil pulse on the radiation intensity. Reduced coordinates, $\omega = 1.78 \cdot 10^{15}$ s^{-1}; the solid line denotes the computed curve, $\tau = 10$ ns.[75,76] Experiment[32]: $\tau = 7.5$ ns; 1—Zn, 2—Al.

[22)]We emphasize that even though the radiation absorption coefficient in such a plasma is small, the extent of the flame is large, so that its optical thickness becomes of the order of unity, which leads to the stationary nature of the vaporization regime.

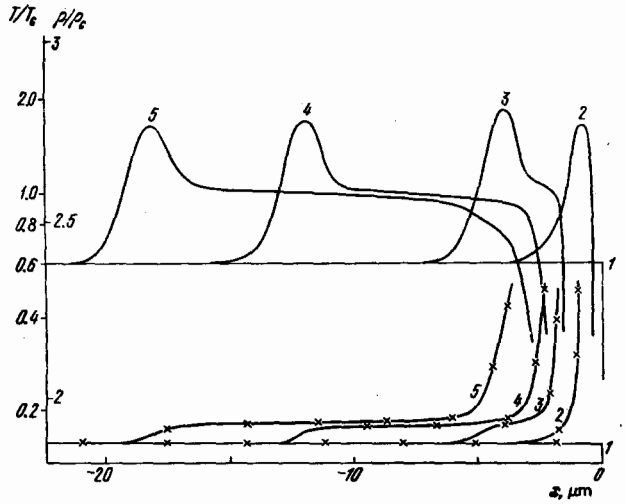

FIG. 22. Computed density (–) and temperature (×) profiles at different times. Rectangular pulse, $\tau = 10$ ns; $\omega = 1.78 \cdot 10^{15}$ s^{-1}; $q = 1$ GW/cm^2. t(ns) = 0 (1), 1 (2), 3 (3), 7.5 (4), and 11 (5).[77]

integrated without any simplifying assumptions. The profiles of temperature and density, obtained in this work, are shown in Fig. 22. The formation of the shock wave and its motion into the bulk of the substance can be easily seen. The width of the layer of the substance compressed by the shock wave increases with time, inasmuch as the shock wave moves at a greater velocity than the stress-relieving wave. From the instant that the shock wave separates from the stress-relieving wave, the structure of the absorbing layer becomes quasistationary. The nonstationary solution quickly passes into the stationary regime, which demonstrates the stability of the latter.

In summarizing the remarks made above, we conclude that the possibilities for experimental observation of the metal-dielectric transition, caused by the action of laser radiation on a metal, are very limited. Indeed, the presence of a dielectric phase should have no effect on the results of indirect experiments (measurement of the effective heat of vaporization and the specific recoil pulse). For this reason, the only way to make such an observation is to observe the "transparency" effect directly. Here, there are two realistic approaches. The first is to study the function $K(z)$ in the expanding flame by probing the flame with a thin beam from an auxiliary laser in a direction that is perpendicular to the propagation of the primary laser beam. As far as we are aware, this approach has not been used. However, it should be emphasized that obtaining reliable results by this method is accompanied with great difficulties due to the small thickness of the dielectric layer and the multidimensional expansion of the focal spot on the periphery, which distorts the results of measurments.

The second approach was used in Refs. 86 and 87, and reduces to the action of radiation on a thin metallic film. In this case, a large part of the metal can become a dielectric and the target becomes completely "transparent." It is also useful in this case to use a weak probing beam with a different frequency, but acting this time in the direction of propagation of the primary beam, as done in Ref. 86 (the transmission of the characteristic ultraviolet radiation of the plasma flame through the foil was studied in Ref. 87). In this case, in correspondence to the previous remarks, the higher the frequency of the probing radiation, the earlier is the onset of the transparency effect for this radiation. The main difficulty in this method lies in the fact that it is difficult to determine whether the "transparency" is due to the metal-dielectric transition in the supercritical region or simply as a result of the evaporation of metal and the trivial transition to a nonconducting gas phase. In our opinion, the available experimental facts are not sufficient to give a unique answer to this question.

We note, however, that in order to attain critical values for the substance, it is not necessary to use only a laser pulse. Thus, for example, a thin metallic film can be placed in a helium atmosphere.[23)] In this case, the helium can first be compressed to a pressure that exceeds the critical pressure for the metal being studied (for cesium, for example, $p_C = 120$ bar,[72] so that there are no particular serious difficulties in setting up this experiment). But, then, with the action of the laser radiation the substance in the target will be known to be in a supercritical state, so that any questions concerning the nature of the transparency can be uniquely answered. However, as far as we are aware, such experiments have not been performed.

7. SOME PROBLEMS. CONCLUSION

As evident from this review, the physics of the interaction of powerful radiation fluxes with a liquid is quite varied, and the phenomena that arise in this case have not by any means been studied completely, either theoretically or experimentally. We have constantly tried to direct the reader's attention toward the appropriate "white spots," more precisely, toward those spots that we could notice. However, our remarks concern the most varied phenomena and occur in various parts of the review. For this reason it is useful to repeat here the most important observations, and also to indicate some of the most interesting problems (in our view) that it was not possible for us to discuss.

First, this includes the group of problems related to the optothermodynamic critical point for a metastable and absolutely unstable liquid that requires thorough theoretical and experimental study.

A comparatively large quantity of interesting experimental material concerning optical breakdown in liquids[24)] and prebreakdown phenomena[88-108] exists si-

[23)]Helium is convenient because it has a high ionization potential, and for this reason, the degree of its ionization during the laser pulse will be small so that this will not distort the picture of the interaction of radiation with the target.

[24)]We note expecially the method of high-speed holography, used in Ref. 109 for studying the dynamics of optical breakdown in a liquid and the accompanying phenomena. Holographic recording allows separating out the output signal from the intense background noise, caused by the scattering of laser radiation on cavitation bubbles and white light from the breakdown region.

multaneously with the most rudimentary state in the theory of this phenomenon, for which only a few references are available and these are concerned mainly with describing the propagation and evolution of the shock wave that arises with breakdown.[110-112]

The "vaporization" mechanism for generating sound has been little studied either experimentally or theoretically, in spite of the fact that there is every reason to expect that its significance must increase with an increase in the intensity of laser radiation. For sufficiently large radiation flux densities, the vaporization mechanism must be predominant, which can significantly increase the efficiency for converting radiation energy into acoustical energy.

The very interesting phenomena of photoacoustical cavition[35,113-115] and laser sonoluminescence[116,117] and the optothermodynamic effects arising with the action of radiation on aerosols[118,119] should also be mentioned.

Finally, we note that optothermodynamic effects are by no means limited to the interaction of laser radiation with a liquid. In this respect, solid solutions, in which the characteristic time for the development of an instability, as a rule, is many orders of magnitude greater than the corresponding quantity in liquids, are also interesting. Laser induced ferroelectric phase transitions in crystals and gaseous media have been examined in Ref. 120–123.

In conclusion, the authors consider it their pleasant duty to express their gratitude to S. I. Anisimov, V. A. Gal'burt, M. F. Ivanov, I. E. Poyurovskii and V. I. Fisher, who presented the results of their work[77] prior to publication. The authors are grateful to V. S. Teslenko and L. K. Chistyakova, who helped in compiling the references, as well as to V. M. Podgaetskii for analyzing a variety of experimental data.

[1]A. M. Prokhorov, S. I. Anisimov, and P. P. Pashinin, Usp. Fiz. Nauk **119**, 401 (1976) [Sov. Phys. Usp. **19**, 547 (1976)].
[2]F. V. Bunkin, Pis'ma Zh. Eksp. Teor. Fiz. **19**, 302 (1974) [JETP Lett. **19**, 1751 (1974)].
[3]L. D. Landau and E. M. Lifshits, Statistical Physics. Part 1 [in Russian], Nauka, Moscow (1976).
[4]V. M. Podgaetskiĭ, Zh. Prikl. Spektrosk. **20**, 48 (1974) [J. Appl. Spectrosc. (USSR)].
[5]G. A. Matyushin, L. S. Mel'nikov, V. M. Podgaetskiĭ, and M. I. Tribel'skiĭ, Kvant. Elektron. (Moscow) **4**, 1076 (1977) [Sov. J. Quantum Electron. **7**, 603 (1977)].
[6]F. V. Bunkin, V. M. Podgaetskiĭ, and M. I. Tribel'skiĭ, Zh. Eksp. Teor. Fiz. **75**, 2309 (1978) [Sov. Phys. JETP **48**, 1165 (1978)].
[7]L. É. Rikenglaz, Zh. Tekh. Fiz. **44**, 1125 (1974) [Sov. Phys. Tech. Phys. **19**, 713 (1974)].
[8]Ya. B. Zel'dovich and Yu. P. Raĭzer, Physics of Shock Waves and High-Temperature Hydrodynamic Phenomena [in Russian], Nauka, Moscow (1966).
[9]M. P. Vukalovich, S. L. Rivkin, and A. A. Aleksandrov, Tables of the Thermodynamic Properties of Water and Water Vapor [in Russian], Izd-vo standartov, Moscow (1969).
[10]N. B. Vargaftik, Handbook of the Thermophysical Properties of Gases and Liquids [in Russian], Nauka, Moscow (1972).
[11]V. P. Skripov, Metastable Liquid [in Russian], Nauka, Moscow (1972).
[12]F. V. Bunkin, L. S. Mel'nikov, V. M. Podgaetskiĭ, and M. I. Tribel'skiĭ, Pis'ma Zh. Tekh. Fiz. **5**, 521 (1979) [Sov. Tech. Fiz. Lett. **5**, 212 (1979)].
[13]R. Cole, Underwater Explosions [Russian translation], IL, Moscow (1950).
[14]Yu. Kagan, Zh. Fiz. Khim. **34**, 92 (1960) [Russ. J. Phys. Chem.].
[15]Ya. B. Zel'dovich, Zh. Eksp. Teor. Fiz. **12**, 525 (1942).
[16]A. Kantrowitz, J. Chem. Phys. **19**, 1097 (1951).
[17]H. Wakeshima, *ibid.* **22**, 1614 (1954).
[18]F. C. Collins, Z. Elektrochem. Bd. 59, S. 404 (1955).
[19]B. K. Chakraverty, Colloq. Intern. Centre Nat. Rech. Scient. **152**, 373 (1965).
[20]V. E. Fortov and A. A. Leont'ev, Teplofiz. Vys. Temp. [High Temp. (USSR)] **14**, 711 (1976).
[21]I. M. Lifshits and V. V. Slezov, Zh. Eksp. Teor. Fiz. **35**, 479 (1959) [Sov. Phys. JETP **8**, 331 (1959)].
[22]I. M. Lifshits and Yu. Kagan, Zh. Eksp. Teor. Fiz. **62**, 385 (1972) [Sov. Phys. JETP **35**, 206 (1972)].
[23]J. W. Gibbs, Thermodynamic Works [in Russian], Gostekhizdat, Moscow-Leningrad (1950).
[24]Ya. B. Zel'dovich and O. M. Todes, Zh. Eksp. Teor. Fiz. **10**, 1441 (1940).
[25]A. Z. Patashinskiĭ and V. L. Pokrovskiĭ, Fluctuation Theory of Phase Transitions [in Russian], Nauka, Moscow (1975).
[26]B. Chu and F. J. Schoenes, Phys. Rev. **185**, 219 (1969).
[27]J. S. Langer, Physica. Ser. A, **73**, 61 (1974).
[28]J. E. Hillard, in Spinodal Decomposition in Phase Transformations, Ed. by H. I. Aronson, Amer. Soc. Metals, Metals Park, Ohio (1970).
[29]Yu. V. Afanas'ev and O. I. Krokhin, Zh. Eksp. Teor. Fiz. **52**, 966 (1967) [Sov. Phys. JETP **25**, 639 (1967)].
[30]V. N. Kondrat'ev, PMTF No. 5, 49 (1972).
[31]N. N. Rykalin and A. A. Uglov, Teplofiz. Vys. Temp. [High Temp. (USSR)] **9**, 575 (1971).
[32]S. I. Anisimov, Ya. A. Imas, G. S. Romanov, and Yu. V. Khodyko, The Action of High-Power Radiation on Metals [in Russian], Nauka, Moscow (1970).
[33]N. V. Karlov, B. B. Krynetskiĭ, V. A. Mishin, and A. A. Samokhin, Pis'ma Zh. Eksp. Teor. Fiz. **19**, 111 (1974) [JETP Lett. **19**, 68 (1974)].
[34]F. V. Bunkin, N. V. Karlov, V. M. Komissarov, and G. P. Kuz'min, *ibid.* **13**, 479 (1971) [JETP Lett. **13**, 341 (1971)].
[35]D. C. Emmony, B. M. Geerken, and A. Straijer, Infrared Phys. **16**, 87 (1976).
[36]L. S. Gournay, J. Acoust. Soc. Am. **40**, 1322 (1966).
[37]D. C. Auth, Appl. Phys. Lett. **16**, 521 (1970).
[38]R. I. Scarlet, Phys. Rev. A **6**, 2281 (1972).
[39]H. Eichler and H. Stahl, J. Appl. Phys. **44**, 3429 (1973).
[40]E. V. Ivakin, A. M. Lazuruk, I. P. Petrovich, and A. S. Rubanov, Kvant. Elektron. (Moscow) **4**, 2421 (1977) [Sov. J. Quantum Electron. **7**, 1382 (1977)].
[41]H. Eichler and H. Stahl, Opt. Commun. **6**, 239 (1972).
[42]E. V. Ivakin, A. M. Lazuruk, I. P. Petrovich, and A. S. Rubanov in Abstracts of VII All-Union Conference on Coherent and Nonlinear Optics (Tashkent, 1974) [in Russian], Izd.-vo Mosk. un-ta, Moscow (1976), p. 110.
[43]E. V. Ivakin, A. M. Lazuruk, I. P. Petrovich, A. S. Rubanov, and B. I. Stepanov, Pis'ma Zh. Eksp. Teor. Fiz. **2**, 466 (1976) [*sic*].
[44]F. V. Bunkin and V. M. Komissarov, Akust. Zh. **19**, 305 (1973) [Sov. Phys. Acoust. **19**, 2031 (1973)].
[45]A. I. Bozhkov and F. V. Bunkin, Kvant. Elektron. (Moscow) **2**, 1763 (1975) [Sov. J. Quantum Electron. **5**, 956 (1978)].
[46]S. G. Kasoev and L. M. Lyamshev, Akust. Zh. **23**, 890 (1977) [Sov. Phys. Acoust. **23**, 510 (1977)].
[47]M. A. Isakovich, General Acoustics [in Russian], Nauka, Moscow (1973).
[48]F. V. Bunkin, V. G. Mikhalevich, and G. P. Shipulo, Kvant. Elektron. (Moscow) **3**, 441 (1976) [Sov. J. Quantum Electron. **6**, 238 (1976)].
[49]A. I. Bozhkov, F. V. Bunkin, and L. L. Gyrdev, *ibid.* **3**,

1494 (1976) [6, 809 (1976)].
[50]S. G. Kasoev and L. M. Lyamshev, Akust. Zh. 23, 265 (1977) [Sov. Phys. Acoust. 23, 149 (1977)].
[51]S. V. Egerev and K. A. Naugol'nykh, *ibid* 23, 738 (1977) [23, 422 (1977)].
[52]A. I. Bozhkov, F. V. Bunkin, and A. A. Kolomenskiĭ, Kvant. Elektron. (Moscow) 4, 942 (1977) [Sov. J. Quantum Electron. 7, 536 (1977)].
[53]A. E. Bozhkov, F. V. Bunkin, and A. A. Kolomenskiĭ in Abstracts of Reports at the IV All-Union Conference on Nonresonant Interaction of Optical Radiation with Matter (Leningrad, 1978) [in Russian], GOI Leningrad (1978), p. 85.
[54]F. V. Bunkin, A. I. Malyarovskiĭ, V. G. Mikhalevich, and G. P. Shipulo, *ibid.*, p. 98.
[55]J. Ready, Action of High-Power Laser Radiation [in Russian], Mir, Moscow (1974).
[56]V. P. Garashuk, O. A. Velichko, and V. B. Davydova, Avtomat. Svarka No. 5, p. 31 (1971).
[57]M. S. Baranov, B. A. Vershok, and I. N. Geĭnrikhs, Teplofiz. Vys. Temp. [High Temp. (USSR)] 13, 566 (1975).
[58]M. S. Baranov, B. A. Vershok, and I. N. Geĭnrikhs, Fiz. i Khim. Obrabutki Mater. No. 5, p. 3 (1976).
[59]A. A. Antonov, G. I. Kozlov, V. A. Kuznetsov, and V. A. Masyukov, Kvant. Elektron. (Moscow) 4, 1747 (1977) [Sov. J. Quantum Electron. 7, 990 (1977)].
[60]V. A. Batanov and V. B. Fedorov, Pis'ma Zh. Eksp. Teor. Fiz. 17, 348 (1973) [JETP Lett. 17, 247 (1973)].
[61]N. N. Rykalin, A. A. Uglov, and A. N. Kokora, Laser Pro-Processing of Materials [in Russian], Mashinostroenie, Moscow (1975).
[62]E. V. Locke, E. D. Hoag, and R. A. Hella, IEEE J. Quantum Electron. QE-8, 132 (1972).
[63]E. V. Locke and R. A. Hella, *ibid.* QE-10, 179 (1974).
[64]M. S. Baranov, B. A. Vershok, and I. N. Geĭnrikhs, Fiz. i Khim Obrabotki Mater. No. 4, p. 8 (1976).
[65]M. I. Tribel'skiĭ, "Report at the 52nd seminar on the physics and chemistry of material processing using intense energy fluxes (Moscow, Institute of Metallurgy of the Academy of Sciences of the USSR, November 1974)", Kvant. Elektron. (Moscow) 5, 804 (1978) [Sov. J. Quantum Electron. 8, 462 (1978)].
[66]V. A. Batanov, F. V. Bunkin, A. M. Prokhorov, and V. B. Fedorov, Zh. Eksp. Teor. Fiz. 63, 586 (1972) [Sov. Phys. JETP 36, 311 (1973)].
[67]S. I. Anisimov and A. Kh. Rakhmatulina, Zh. Eksp. Teor. Fiz. 64, 869 (1973) [Sov. Phys. JETP 37, 441 (1973)].
[68]L. D. Landau, and E. M. Lifshits, Mechanics of Continuous Media [in Russian], Gostekhizdat, Moscow (1954).
[69]N. N. Rarov, A. A. Uglov, and I. V. Zuev, Dokl. Akad. Nauk SSSR 207, 83 (1972) [Sov. Phys. Dokl. 17, 1087 (1973)].
[70]J. G. Andrews and D. R. Atthey, J. Phys. D 9, 2181 (1976).
[71]Ya. B. Zel'dovich and L. D. Landau, Acta Phys. Chim. USSR 18, 194 (1943); Zh. Eksp. Teor. Fiz. 14, 32 (1944).
[72]V. A. Alekseev, A. A. Andreev, and V. Ya. Prokhorenko, Usp. Fiz. Nauk 106, 393 (1972) [Sov. Phys. Usp. 15, 1391 (1972)].
[73]I. K. Kikoin and A. P. Senchenkov, Fiz. Met. Metalloved. [Phys. Met. Metallogr. (USSR)] 24, 843 (1967).
[74]F. V. Bunkin, Kvant. Elektron. (Moscow) 1, 2055 (1974) [Sov. J. Quantum Electron. 4, 1143 (1975)].
[75]V. I. Fisher, Author's Abstract of Candidate's Dissertation, Chernogolovka, Institute of Theoretical Physics of the Academy of Sciences of the USSR, 1974.
[76]S. I. Anisimov, V. A. Gal'burt, and V. I. Fisher, Pis'ma Zh. Tekh. Fiz. 1, 321 (1975) [Sov. Tech. Phys. Lett. 1, 153 (1975)].
[77]S. I. Anisimov, V. A. Gal'burt, M. F. Ivanov, I. E. Poyurovskaya, and V. I. Fisher, Zh. Tekh. Fiz. 49, 512 (1979) [Sov. Phys. Tech. Phys. 24, 295 (1979)].
[78]F. V. Bunkin, V. I. Konov, A. M. Prokhorov, and V. B. Fedorov, Pis'ma Zh. Eksp. Teor. Fiz. 9, 609 (1969) [JETP Lett. 9, 371 (1969)].
[79]F. Hansel and E. V. Frank, Rev. Mod. Phys. 40, 697 (1968).
[80]H. Renkert, F. Hensel, and E. V. Frank, Phys. Lett. A 30, 494 (1969).
[81]V. A. Alekseev, V. G. Ovcharenko, Yu. F. Ryzhkov, and A. P. Senchenkov, Pis'ma Zh. Eksp. Teor. Fiz. 12, 306 (1970) [Sov. Phys. JETP 12, 207 (1970)].
[82]Yu. S. Korshunov, A. P. Senchenkov, E. I. Asinovskiĭ, and A. T. Kunavin, Teplofiz. Vys. Temp. [High Temp. (USSR)] 8, 1288 (1970).
[83]V. A. Alekseev and A. A. Vedenov, Usp. Fiz. Nauk 102, 665 (1970) [Sov. Phys. Usp. 13, 830 (1970)].
[84]B. M. Smirnov, Dokl. Akad. Nauk SSSR 195, 75 (1970) [Sov. Phys. Dokl. 15, 1050 (1971)].
[85]V. E. Fortov, A. A. Leont'ev, A. N. Dremin, Teplofiz. Vys. Temp. [High Temp. (USSR)] 13, 1072 (1975).
[86]A. M. Bonch-Bruevich and S. E. Potapov, Pis'ma Zh. Tekh. Fiz. 1, 353 (1975) [Sov. Tech. Phys. Lett. 1, 167 (1975)].
[87]Yu. I. Dymshits, *ibid.* 2, 751 (1976) [2, 294 (1976)].
[88]G. A. Askaryan, A. M. Prokhorov, G. F. Chanturiya, and G. P. Shipulo, Zh. Eksp. Teor. Fiz. 44, 2180 (1963) [Sov. Phys. JETP 17, 1463 (1963)].
[89]R. G. Brewer and K. E. Rieckhoff, Phys. Rev. Lett. 13, 334a (1964).
[90]E. F. Carome, C. E. Moeller, and N. A. Clark, J. Acoust. Soc. Am. 40, 1462 (1966).
[91]S. E. Bell and J. A. Landt, Appl. Phys. Lett. 10, 46 (1967).
[92]P. A. Barnes and K. E. Rieckhoff, *ibid.* 13, 282 (1968).
[93]A. A. Buzukov, Yu. A. Popov, and V. S. Teslenko, PMTF No. 5, 17 (1969).
[94]J. F. Roach, W. Zagiboylo, and J. M. Davies, Proc. IEEE 57, 1693 (1969).
[95]V. S. Teslenko, Kvant. Elektron. (Moscow) 2, 1248 (1975) [Sov. J. Quantum Electron. 5, 676 (1975)].
[96]V. S. Teslenko, *ibid.* 4, 1732 (1977) [8, 981 (1977)].
[97]H. Fujii, K. Yoshino, and Y. Inuishi, Technol. Repts. Osaka Univ. 26, No. 1319, 461 (1976); J. Phys. D., 10, 1975 (1977).
[98]A. V. Butenin, and B. Ya. Kogan, Pis'ma Zh. Tekh. Fiz. 3, 433 (1977) [Sov. Tech. Phys. Lett. 3, 175 (1977)].
[99]A. A. Buzukov and V. S. Teslenko, PMTF No. 3, p. 123 (1970).
[100]A. I. Ioffe, N. A. Mel'nikov, K. A. Naugol'nykh, and V. A. Upadyshev, *ibid.*, p. 125.
[101]R. K. Leonov, N. F. Taurin, K. B. Sherstnev, and P. A. Yampol'skiĭ, Fiz. i Khim. Obrabotki Mater. No. 6, p. 134 (1974).
[102]R. K. Leonov, V. V. Efimov, S. I. Zakharov, N. F. Taurin, and P. A. Yampol'skiĭ, Zh. Tekh. Fiz. 45, 130 (1975) [Sov. Phys. Tech. Phys. 20, 197 (1975)].
[103]V. S. Teslenko, PMTF No. 4, p. 109 (1976).
[104]V. S. Teslenko, cited in ref. 53, p. 335.
[105]R. Yu. Orlov, I. P. Skidan, and L. S. Telegin, Zh. Eksp. Teor. Fiz. 61, 784 (1971) [Sov. Phys. JETP 34, 418 (1972)].
[106]A. V. Butenin and B. Ya. Kogan in Quantum Electronics [in Russian], Ed. by N. G. Basov, Sov. Radio, Moscow (1971), No. 5, p. 143.
[107]P. I. Bal'kyavichyus, E. K. Kosenko, I. P. Lukoshyus, and E. K. Maldutis, cited in Ref. 53, p. 59.
[108]S. Z. Arushanov, V. N. Kosolobov, V. M. Mizin, and Yu. G. Khronopulo, *ibid.*, p. 48.
[109]W. Lauterborn and L. K. Ebeling, Appl. Phys. Lett. 31, 663 (1977).
[110]S. I. Zakharov, Yu. N. Lokhov, and Yu. L. Fiveĭskiĭ, Fiz. i Khim. Obrabotki Mater. No. 4, p. 16 (1974).
[111]S. V. Egerev, I. B. Esipov, and K. A. Naugol'nykh, cited in Ref. 53, p. 170.
[112]A. L. Kupershtokh and V. S. Teslenko, *ibid.*, p. 245.
[113]F. V. Bunkin, V. I. Konov, A. M. Prokhorov, V. V. Savranskiĭ, and V. B. Fedorov, Zh. Eksp. Teor. Fiz. 67, 2087 (1974) [Sov. Phys. JETP 40, 1036 (1975)].

[114]V. M. Rysakov and V. I. Korotkov, Kvant. Elektron. (Moscow) 2, 1087 (1975) [Sov. J. Quantum Electron. 5, 595 (1975)].
[115]T. A. Dunina, S. V. Egerev, and K. N. Naugol'nykh in Symposium on the Physics of Hydroacoustic Phenomena: Collection of Reports (Sukhumi, 1975), Moscow (1975), p. 98.
[116]A. A. Bazukov and V. S. Teslenko, Pis'ma Zh. Eksp. Teor. Fiz. 14, 286 (1971) [JETP Lett. 14, 189 (1971)].
[117]A. G. Akmanov, V. G. Ben'kovskiĭ, P. I. Golubnichiĭ, S. I. Maslennikov, and V. G. Shemanin, Akust. Zh. 19, 649 (1973) [Sov. Phys. Acoust. 19, 417 (1973)].
[118]N. V. Bukzdorf, A. A. Zemlyanov, A. V. Kuzikovskiĭ, and S. S. Khmelevtsov, Izv. Vyssh. Uchebn. Zaved. Fiz. [Sov. Phys. J.] No. 5, p. 36 (1974).
[119]A. V. Kuzikovskiĭ and L. K. Chistyakova in Abstracts of Reports at the IV All-Union Symposium on Propagation of Laser Radiation in the Atmosphere, Tomsk Institute of Atmospheric Optics, Siberian Division of the Academy of Sciences of the USSR (1970), p. 10.
[120]V. I. Emel'yanov and Yu. L. Klimontovich, Kvantovaya Elektron. (Moscow) 3, 848 (1976) [Sov. J. Quantum Electron. 3, 462 (1976)].
[121]V. I. Emel'yanov, Fiz. Tverd. Tela (Leningrad) 19, 3312 (1977) [Sov. Phys. Solid State 19, 1934 (1977)].
[122]V. I. Emel'yanov and Yu. L. Klimontovich, Pis'ma Zh. Eksp. Teor. Fiz. 27, 7 (1978) [JETP Lett. 27, 4 (1978)].
[123]V. I. Emel'yanov and Yu. L. Klimontovich, cited in ref. 53, p. 174.
[124]P. G. Klemens, J. Appl. Phys. 47, 2165 (1976).
[125]V. P. Skripov and A. V. Skripov, Usp. Fiz. Nauk 128, 193 (1979) [Sov. Phys. Usp. 22, 389 (1979)].
[126]A. A. Vedenov, G. G. Gladush, and A. N. Yavokhin in Abstracts of the Fifth All-Union Conference on the Physics of Low-Temperature Plasma, Vol. I, Kiev, 1979.
[127]S. I. Anisimov, M. I. Tribel'skiĭ, and Ya. G. Épel'baum, Zh. Eksp. Teor. Fiz. 78, 1597 (1980) [Sov. Phys. JETP 51, in press (1980)].
[128]S. P. Kaznovskiĭ, Yu. F. Selivanov, V. I. Subbotin, and N. N. Shan'gin, Teplofiz. Vys. Temp. [High. Temp. (USSR)] 14, 1007 (1976).
[129]A. V. Burmistrov, PMTF No. 3, p. 35 (1979).

Translated by M. E. Alferieff